

Contract No:

This document was prepared in conjunction with work accomplished under Contract No. 89303321CEM000080 with the U.S. Department of Energy (DOE) Office of Environmental Management (EM).

Disclaimer:

This work was prepared under an agreement with and funded by the U.S. Government. Neither the U.S. Government or its employees, nor any of its contractors, subcontractors or their employees, makes any express or implied:

- 1) warranty or assumes any legal liability for the accuracy, completeness, or for the use or results of such use of any information, product, or process disclosed; or
- 2) representation that such use or results of such use would not infringe privately owned rights; or
- 3) endorsement or recommendation of any specifically identified commercial product, process, or service.

Any views and opinions of authors expressed in this work do not necessarily state or reflect those of the United States Government, or its contractors, or subcontractors.

Defect-related carrier transport in CdTe-based compounds: comparison with hybrid perovskites

Jan Franc¹, Václav Dědič¹, Roman Grill¹, Martin Rejhon^{1,2},
Eduard Belas¹, Jindřich Pipek¹, Petr Praus, Utpal N. Roy³,
Ralph James³ and Paul Sellin⁴

- 1) Faculty of Mathematics and Physics, Charles University, Ke
Karlovu 5, CZ-121 16, Prague 2, Czech Republic
- 2) Tandon School of Engineering, New York University,
Brooklyn, NY 11201, USA
- 3) Savannah River Natl Lab, Aiken, SC 29808 USA
- 4) Univ Surrey, Dept Phys, Guildford GU2 7XH, Surrey,
England

Thanks:

Group in Prague:

V. Dědič, M. Rejhon , R. Grill, E. Belas, P. Moravec, P. Höschl, P. Praus, J. Pipek,
M. Betušiak, R. Fesh, J. Kubát, H. Elhadidy

Main collaborating groups:

- Brookhaven National Laboratory, R.B. James, U. N. Roy, K.H.Kim, A. Bolotnikov, Ge Yang, R.Gul, G. Camarda
- Savannah River National Laboratory – R.B. James, U. N. Roy
- Freiburger Materialforschungszentrum (FMF) – M. Fiederle, A. Fauler, V. Babentsov
- University of Surrey – P. Sellin
- IMEM, Parma – A. Zappettini
- University of Bologna – B. Fraboni, A. Cavallini
- Korea University – K.H.Kim
- Redlen technologies – G. Prekas, K. Iniewski

History of CdTe crystal growth and defect studies at the Institute of Physics, Charles University

1962 – 1st paper (Growing of CdTe single crystals by static sublimation.., P.Höschl, C.Konak, Czech.J.Phys.)

1977 –paper P. Höschl et al., Rev.Phys.Appl.



1985 –2002 HgCdTe bulk crystals for infrared detectors
CdZnTe crystals as substrates for HgCdTe MBE
epitaxial layers

CdTe

CdZnTe

CdZnTeSe

For X-ray and gamma-ray detectors

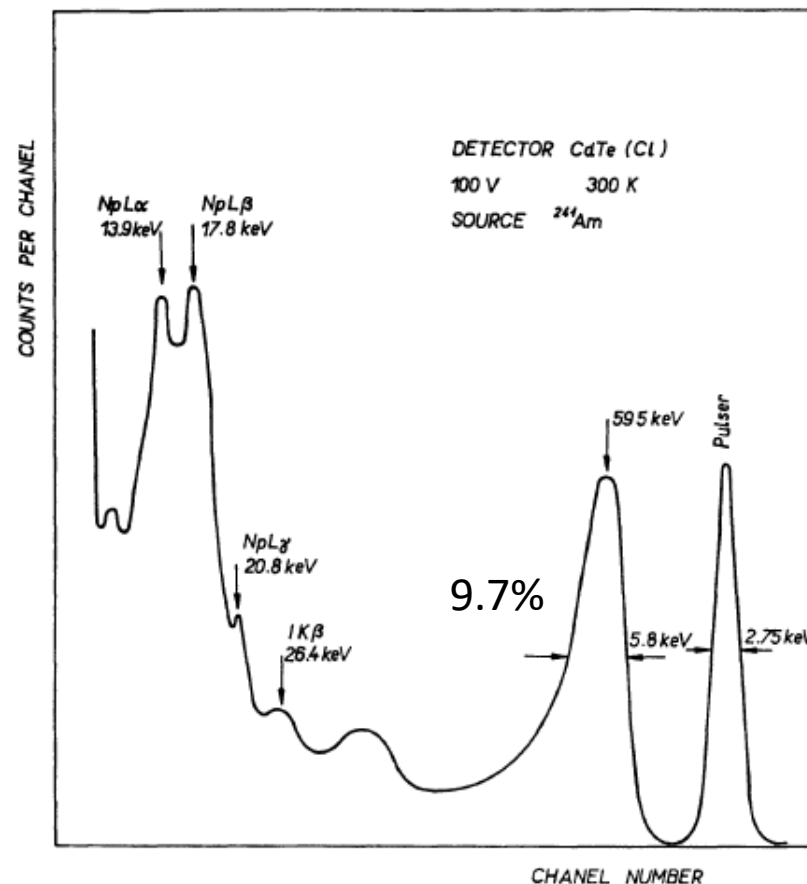


FIG. 5. — ^{241}Am gamma-ray spectrum at room temperature.

Defects and their impact on detector performance

Methods

photoluminescence

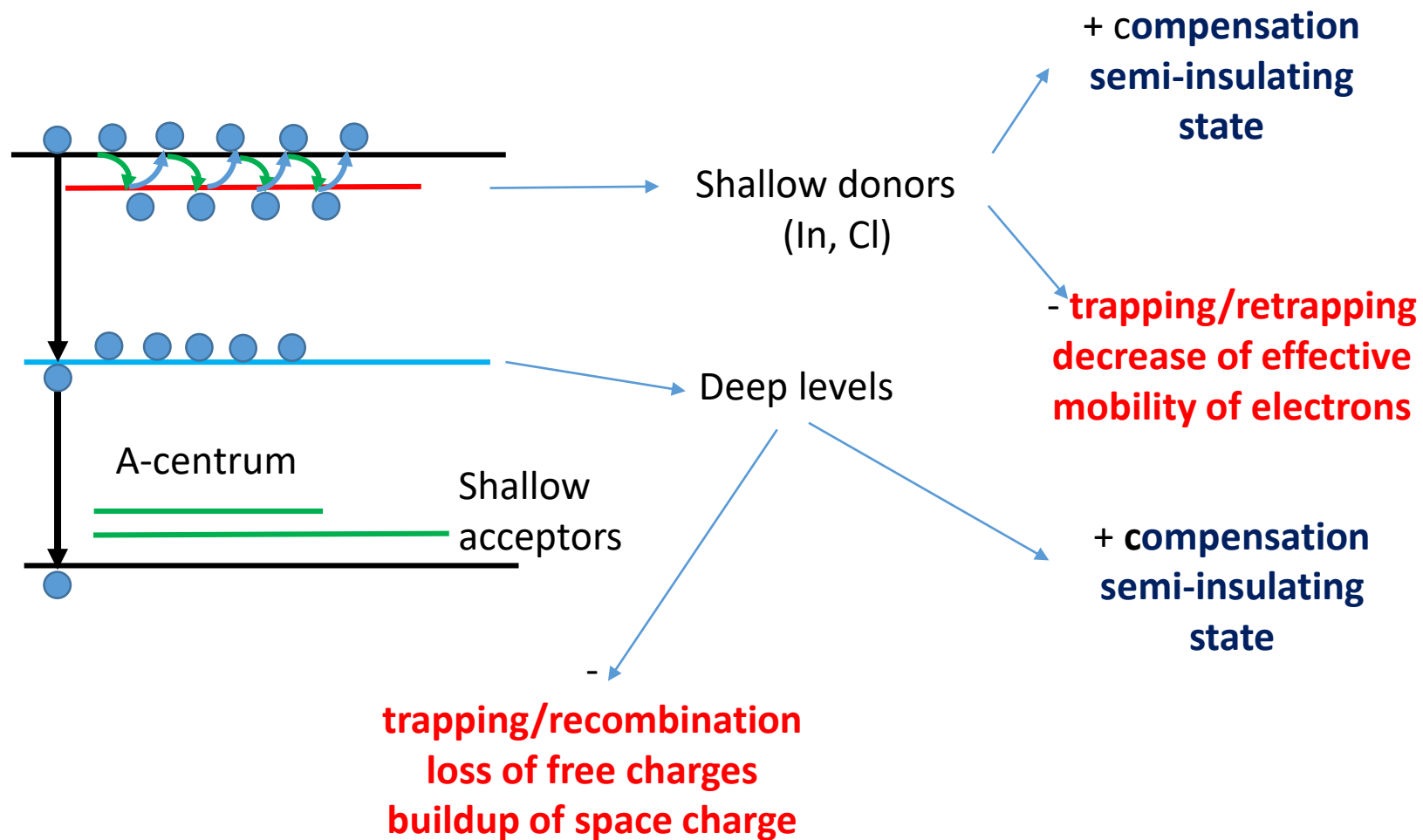
TEES, PICTS

photoconductivity

Pockels effect

Transient current technique
(L-TCT)

Photo-Hall effect spectroscopy



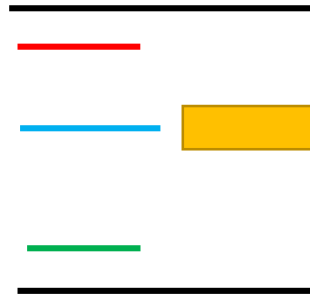
Achievement of the semi-insulating state

$$N_D \sim 10^{15} \text{ cm}^{-3}$$

$$N_{DEEP} \sim 10^{11} \text{ cm}^{-3}$$

$$\sigma \sim 10^{-13} - 10^{-14} \text{ cm}^2$$

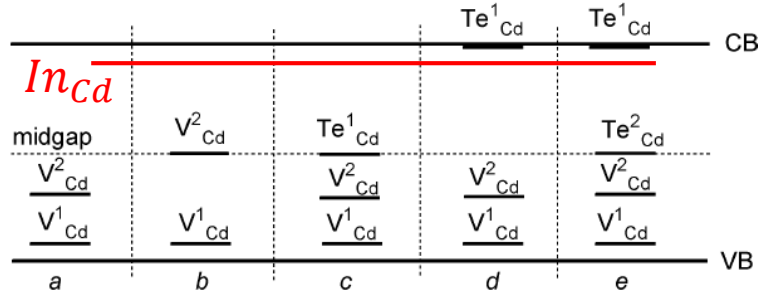
$$N_A \sim 10^{15} \text{ cm}^{-3}$$



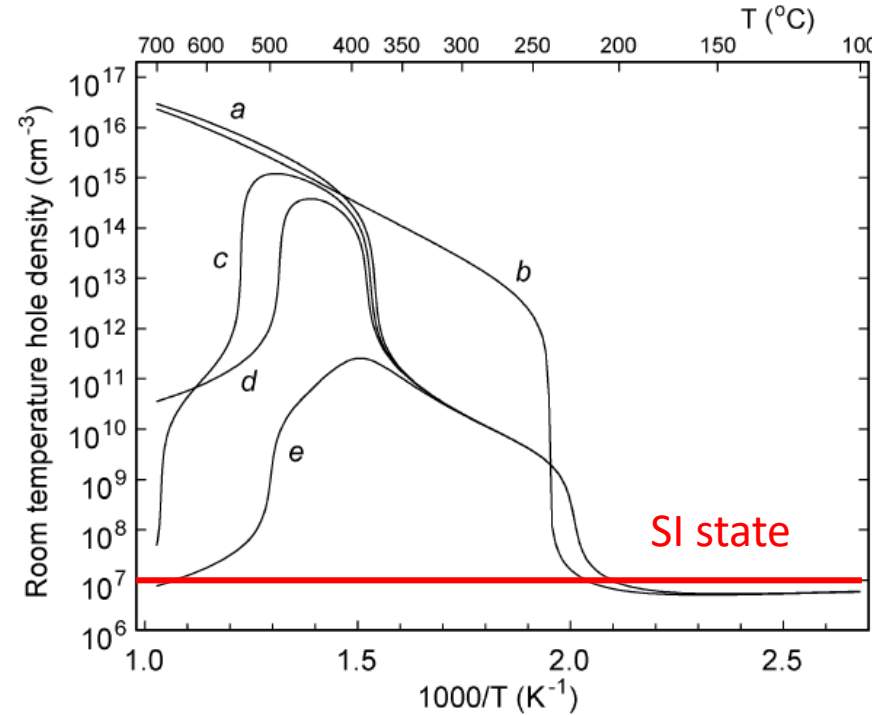
Fermi energy



$$N_{DEEP} > |N_D - N_A| \text{ cm}^{-3}$$



R. Grill, J. Franc, P. Höschl, I. Turkevych, E. Belas, P. Moravec, IEEE Trans. Nucl. Sci. 52, 1925, 2005.



$$V_{Cd}, Te_{Cd} \rightarrow Te_{ppt}$$

Model

Slow cooling at Te-rich conditions

Reduction of point defects by precipitation

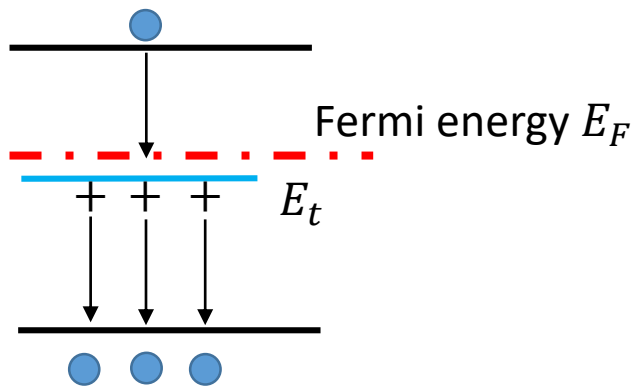


Semi-insulating state is achieved at ~200K

Midgap level

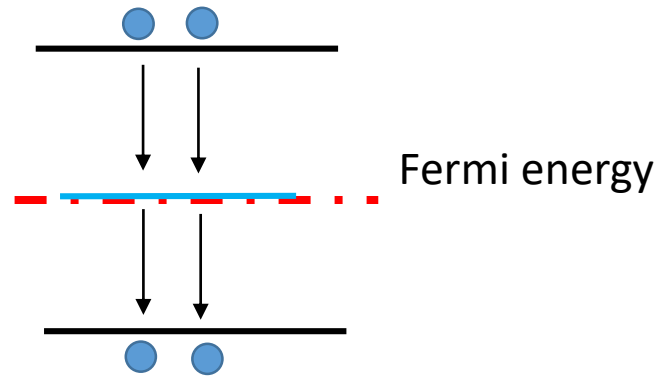
$$\tau_{t,e} = \frac{1}{\sigma_e v_{th} N_t f} \quad f = \frac{1}{1 + e^{E_t - E_F}}$$

Weak N-type



Weak electron trapping,
Good electron mobility

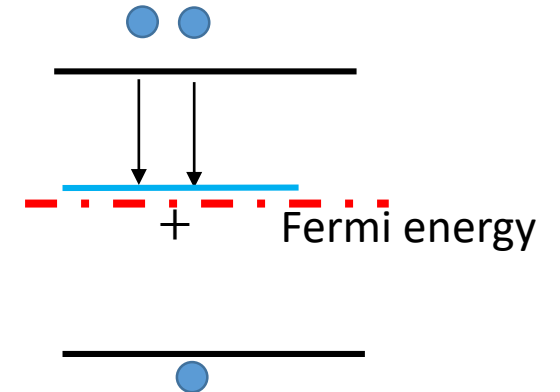
Strong hole trapping,
Buildup of positive
space charge



Recombination center

Due to a higher electron than hole
mobility trapping of electrons is weaker
than the trapping of holes

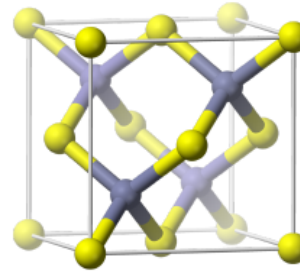
Weak P-type



Moderate electron trapping
Weak hole trapping

Electric field measurements – Pockels effect

CdTe, CdZnTe, CdZnTeSe ... optically isotropic crystals of $\bar{4}3m$ symmetry (FCC) showing Pockels effect (E-field induced birefringence)



E-field	Crystal
0	isotropic
$\neq 0$	anisotropic

Taylor:

$$n(E) = n + a_1 E + \frac{1}{2} a_2 E^2 + \dots$$

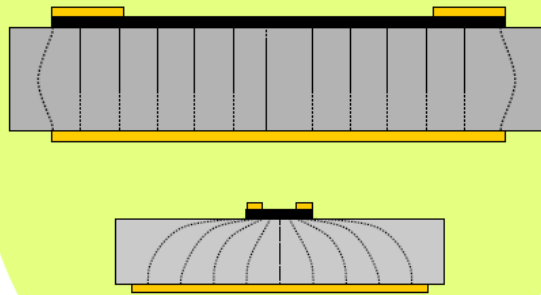
with electrooptic coefficients r and s :

$$n(E) \approx n - \frac{1}{2} r n^3 E - \frac{1}{2} s n^3 E^2$$

Pockels effect
(linear)

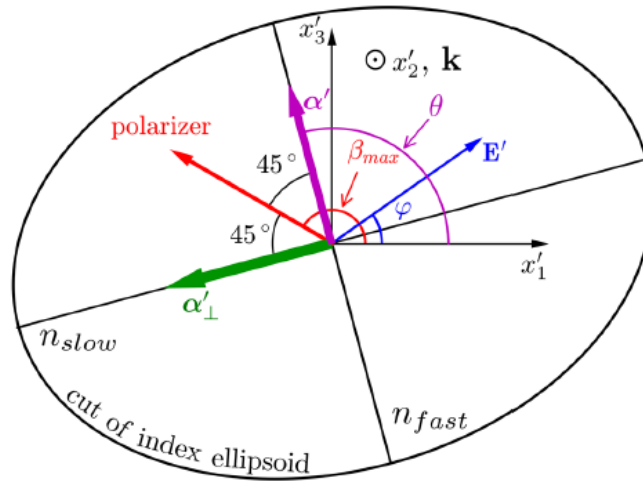
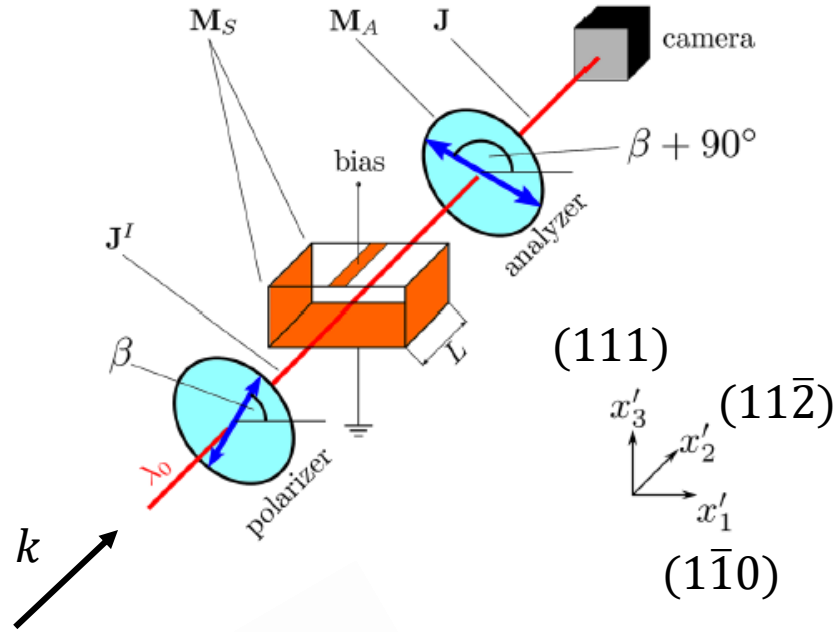
Kerr effect
(quadratic)

E-field ?



Gauss law: E-field \iff space charge

Pockels effect – arbitrary direction of E-field



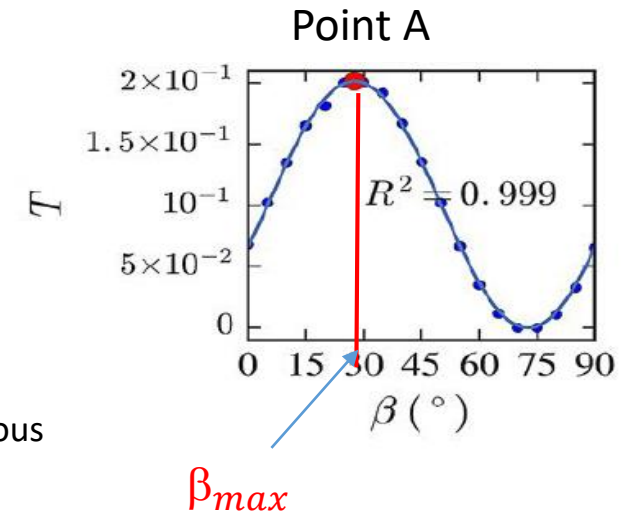
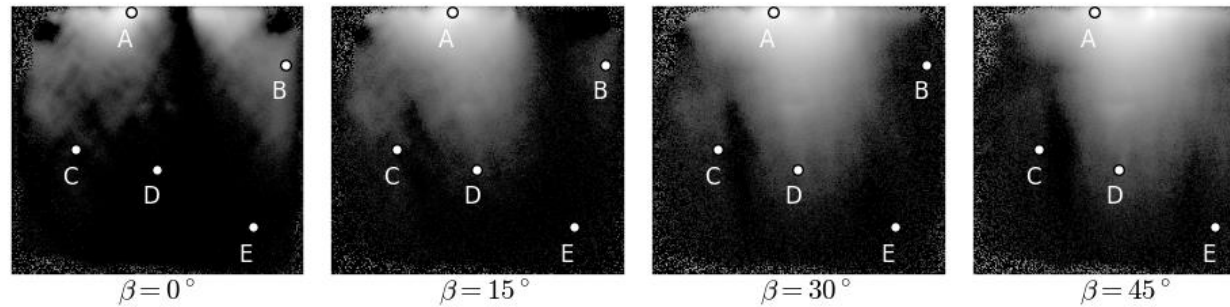
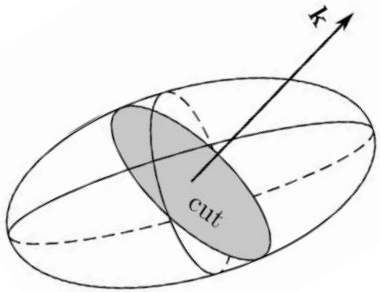
We measure transmission

$$T(E) = \sin^2 \frac{\Gamma(E)}{2} \sin^2 [2(\beta - \theta)]$$

$$\Gamma(E) = \frac{2\pi}{\lambda_0} [n_{fast} - n_{slow}] L$$

$$T_{max}(E) = \sin^2 \frac{\Gamma(E)}{2}$$

$$T_{max}(E, \varphi) = \sin^2 \left(\frac{\pi}{\lambda_0} n_0^3 r_{41} L E \left| \frac{\cos(2\beta_{max} - \varphi) - 5 \cos(2\beta_{max} + \varphi)}{4\sqrt{3}} \right| \right).$$

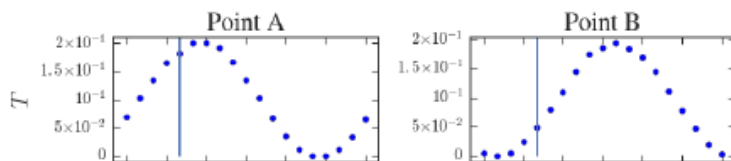
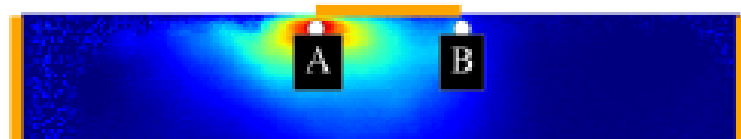
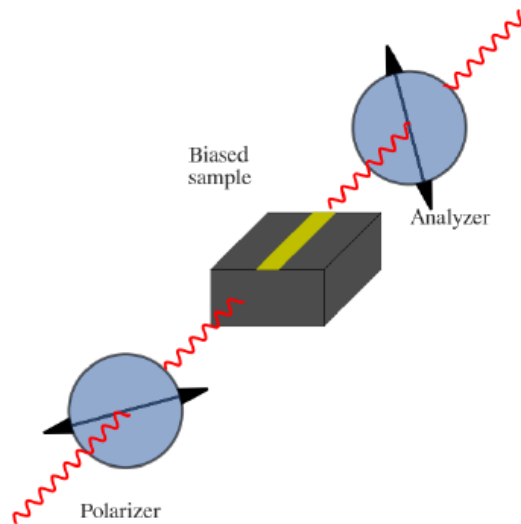


Václav Dědič, Tomáš Fridrišek, Jan Franc, Jan Kunc, Martin Rejhon, Utpal N. Roy, Ralph B. James, Mapping of inhomogeneous quasi-3D electrostatic field in electro-optic materials, Scientific Reports (2021) 11:2154

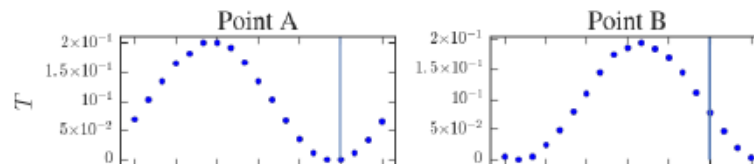
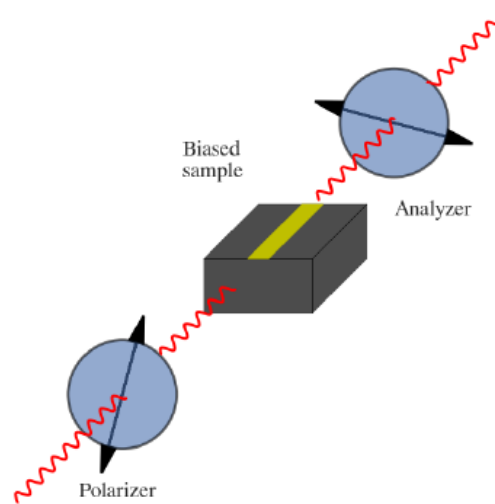
RTSD Workshop, Milano, November 10, 2022

Mapping of electric fields

Polarizer angle $\beta = 15^\circ$



Polarizer angle $\beta = 75^\circ$

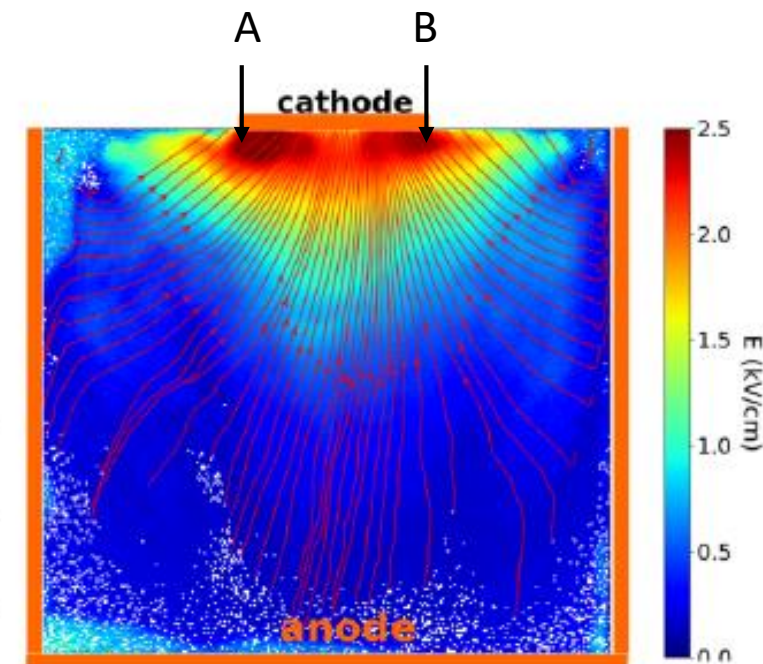


$$T(E) = \sin^2 \frac{\Gamma(E)}{2} \sin^2 [2(\beta - \theta)]$$

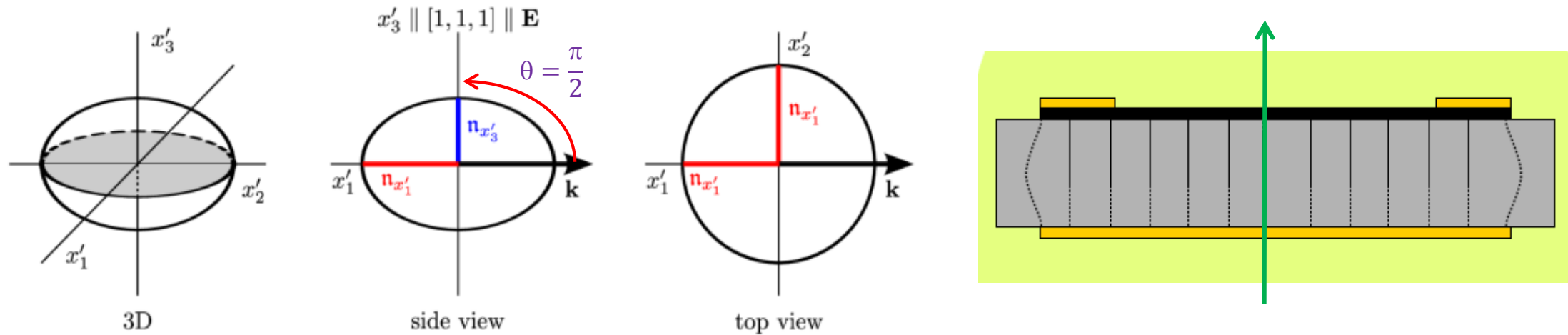
Evaluation of the E-field map:

1. Each pixel must be treated as a separate sample
2. Maximum of transmission T is found rotating the crossed polarizer-analyzer set
3. E-field calculated from

$$T_{max}(E) = \sin^2 \frac{\Gamma(E)}{2}$$



Pockels effect – E-field is parallel to (111)

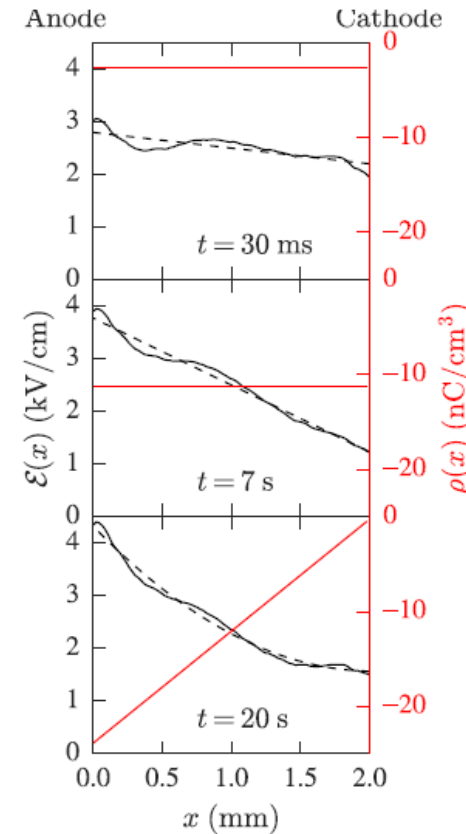
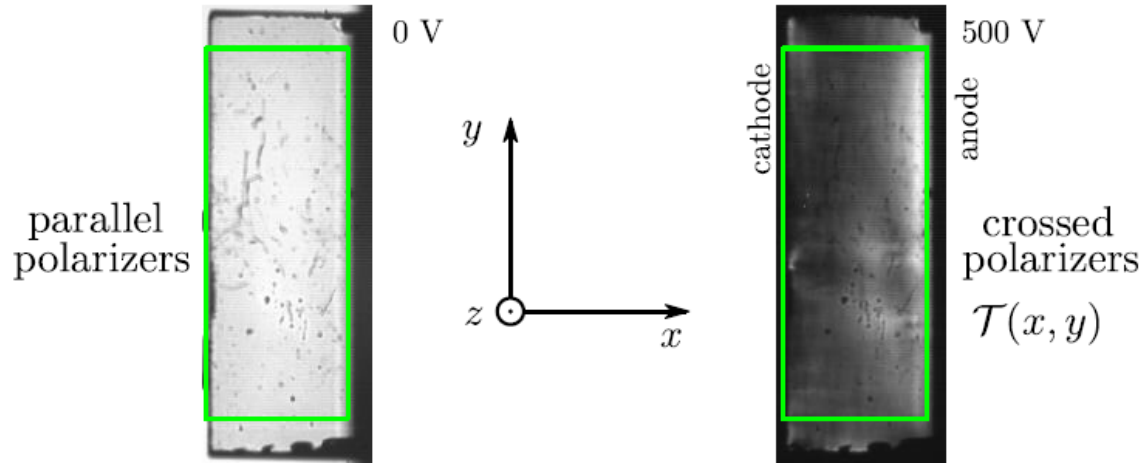
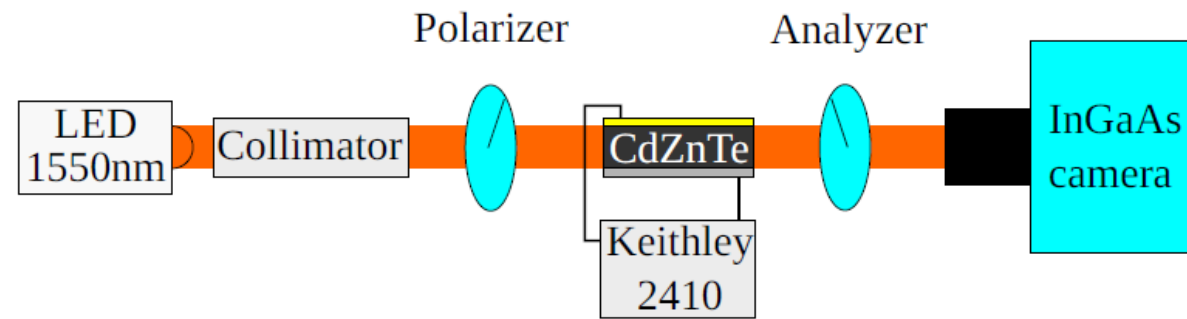


$$\theta = \frac{\pi}{2}, \text{ for } \beta = \frac{\pi}{4} \Rightarrow 2(\beta - \theta) = -\frac{\pi}{2} \Rightarrow \sin^2[2(\beta - \theta)] = 1 \Rightarrow T(E) = T_{max}(E) = \sin^2 \frac{\Gamma(E)}{2}$$

Simple situation, with polarizer angle $\beta = \frac{\pi}{4}$, analyzer angle $\beta = \frac{3\pi}{4}$, T_{max} is measured

Electric field evaluation

$$T = \sin^2 \left(\frac{\sqrt{3}}{2} \frac{\pi r_{41} n_0^3 E L}{\lambda_0} \right) \Rightarrow E(x'_1, x'_3) = \frac{2}{\sqrt{3}} \frac{\lambda_0}{\pi r_{41} n_0^3 L} \arcsin \sqrt{T(x'_1, x'_3)} = \alpha_P \arcsin \sqrt{T(x'_1, x'_3)}$$



Space charge density

$$\rho(x) = \epsilon \frac{\partial \mathcal{E}(x)}{\partial x}$$

Total space charge

$$Q = \int_V \rho(x) dV = S \int_a^c \rho(x) dx$$



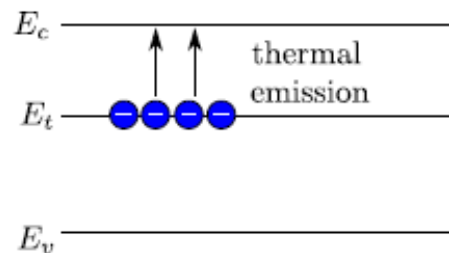
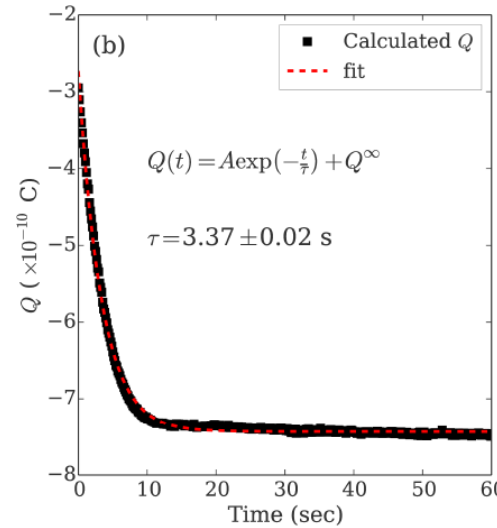
$$Q = \epsilon S (\mathcal{E}_c - \mathcal{E}_a)$$

Experimental methods based on Pockels effect I

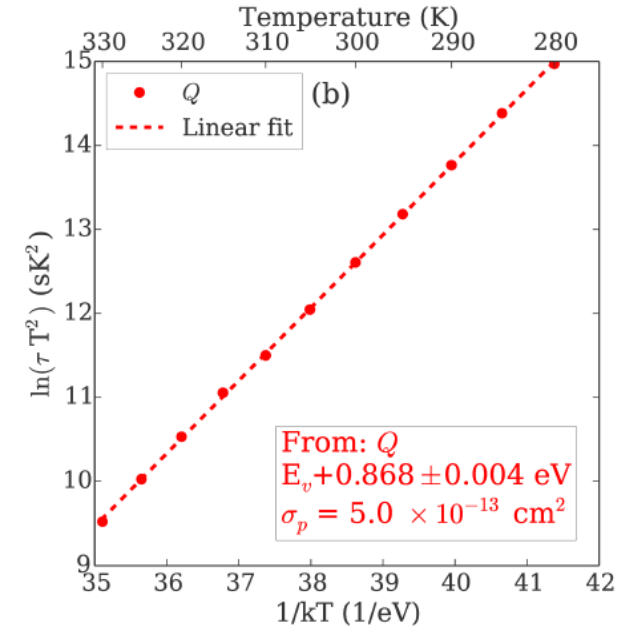
E-field DLTS

(DLTS = deep level transient spectroscopy)

- Subject of study: thermal emission of carriers from traps
- Temporal and temperature dependence of the E-field (reflecting space charge) after switchin ON the bias or switching OFF the illumination (light assisted trap filling)
- Output: activation energy and capture cross-sections of traps (Arrhenius plot) \Rightarrow deep levels responsible for space charge accumulation
- Advantage: higher sensitivity than current techniques, direct space charge sign estimation



$$Q(t) = A \exp\left(-\frac{t}{\tau}\right) + Q^\infty.$$



Arrhenius equation: $\ln(\tau T^2) = \frac{E}{kT} + \ln\left(\frac{C}{\sigma}\right)$ $C = \frac{h^3}{16m_{e(h)}^* \pi k_B^2}$

Determination of type of transitions

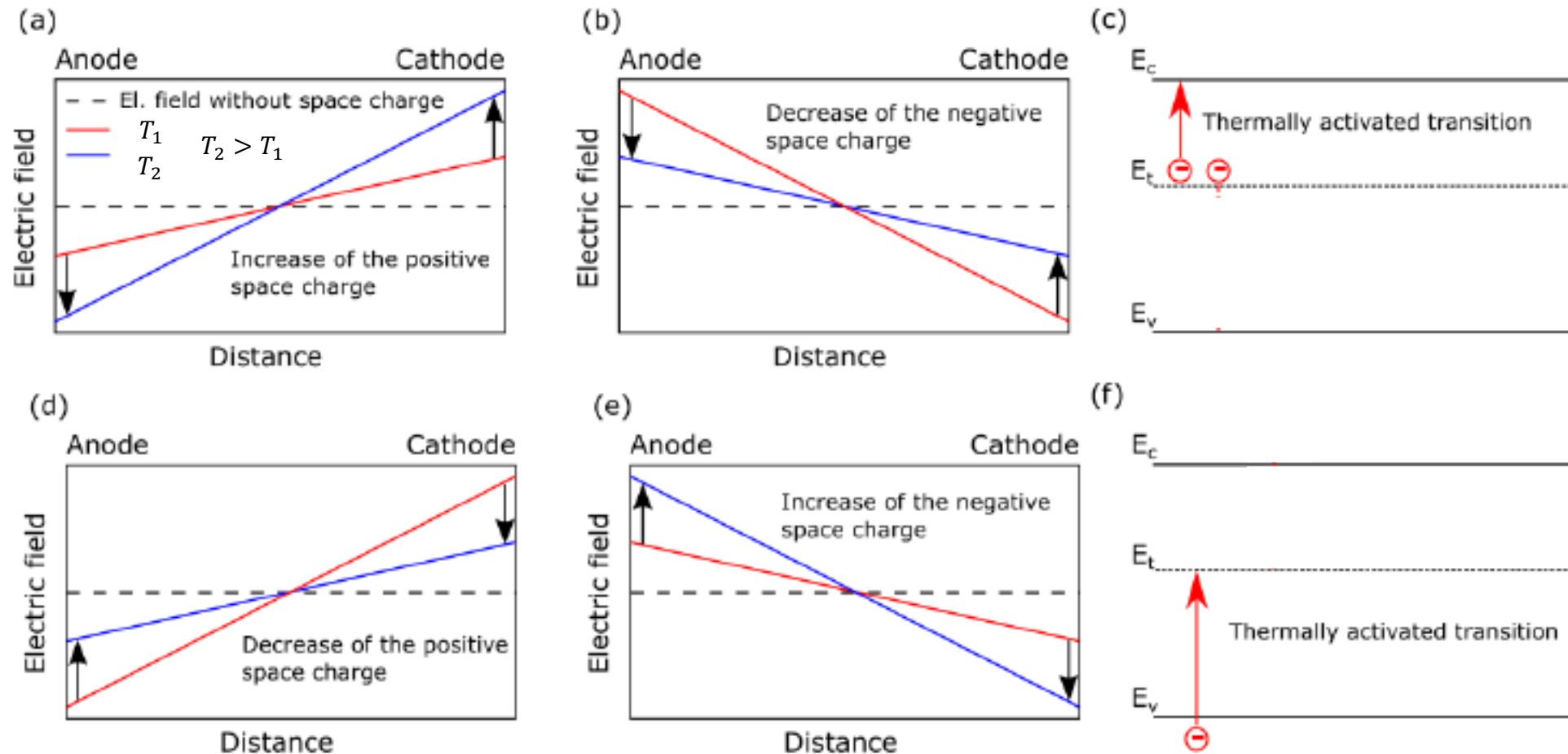
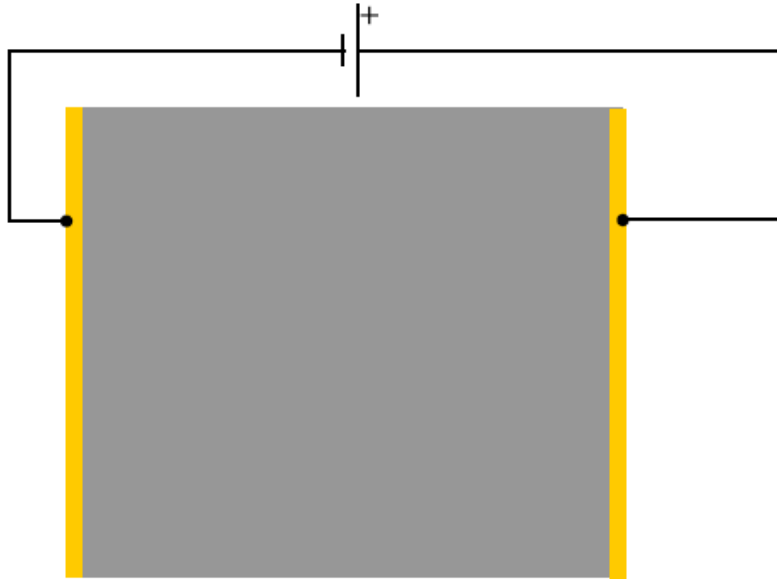


Photo generated space charge

Example (biased semiinsulating sample):

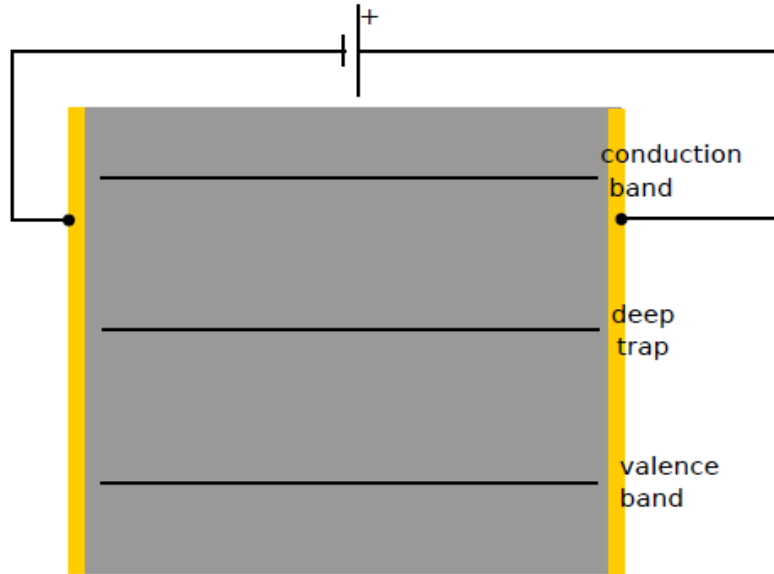


Main factors:

- defect structure (traps, optical transitions)
- penetration depth (photon energy)
- polarity (in case of low penetration)
- electrode material

Photo generated space charge

Example (biased semiinsulating sample):

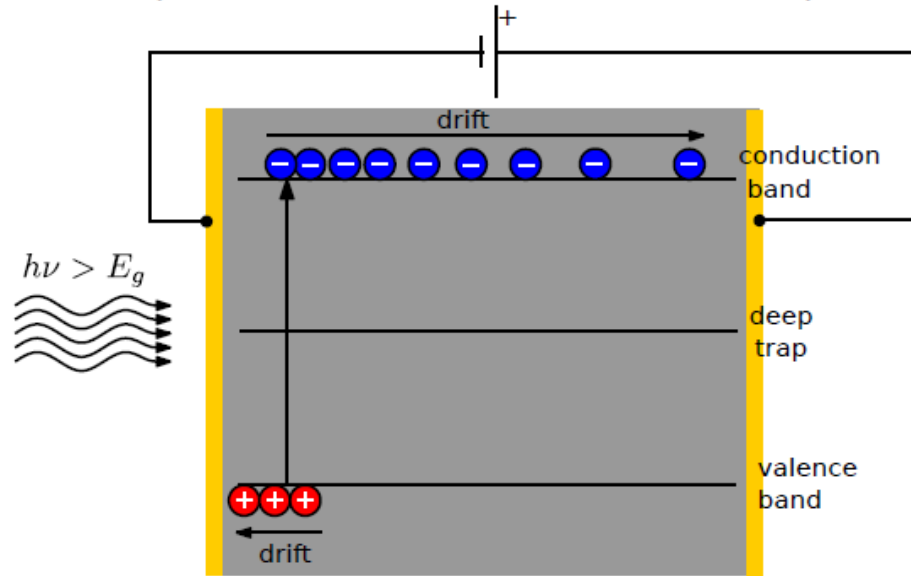


Main factors:

- defect structure (traps, optical transitions)
- penetration depth (photon energy)
- polarity (in case of low penetration)
- electrode material

Photo generated space charge

Example (biased semiinsulating sample):

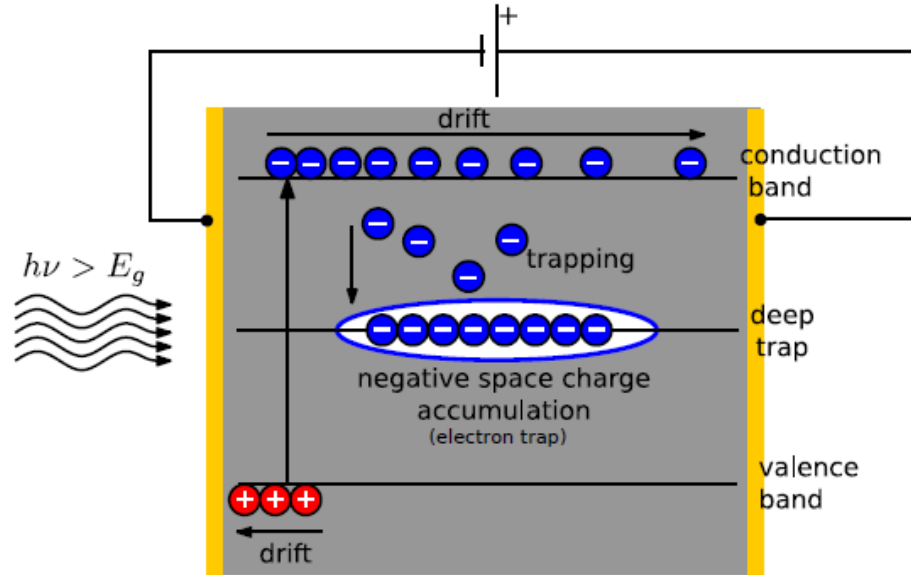


Main factors:

- defect structure (traps, optical transitions)
- penetration depth (photon energy)
- polarity (in case of low penetration)
- electrode material

Photo generated space charge

Example (biased semiinsulating sample):

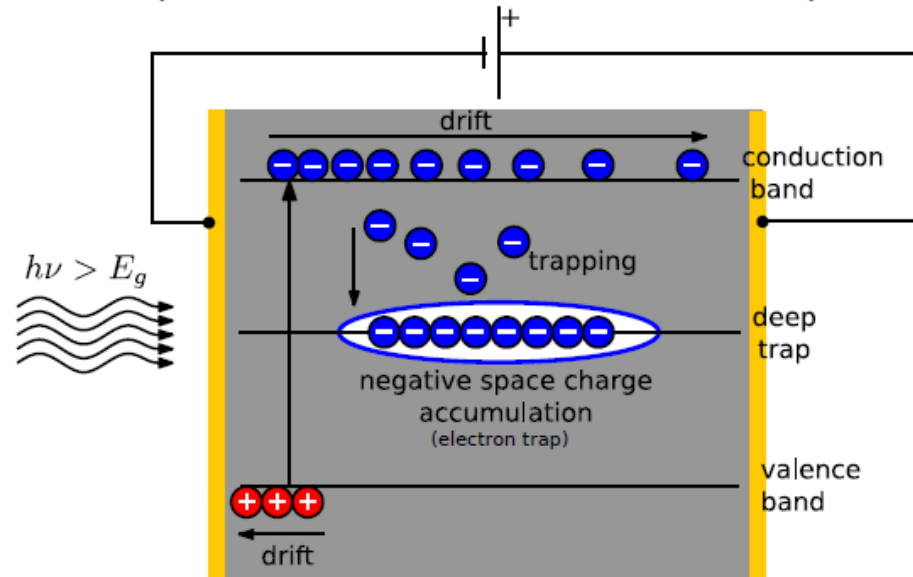


Main factors:

- defect structure (traps, optical transitions)
- penetration depth (photon energy)
- polarity (in case of low penetration)
- electrode material

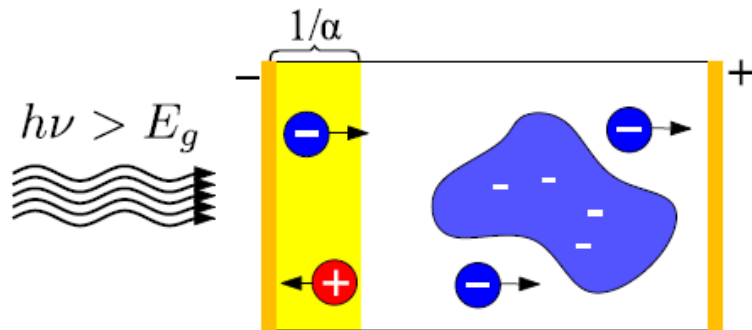
Photo generated space charge

Example (biased semiinsulating sample):

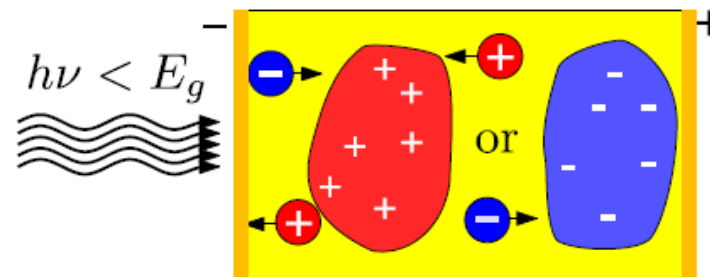


Main factors:

- defect structure (traps, optical transitions)
- penetration depth (photon energy)
- polarity (in case of low penetration)
- electrode material



depends on polarity

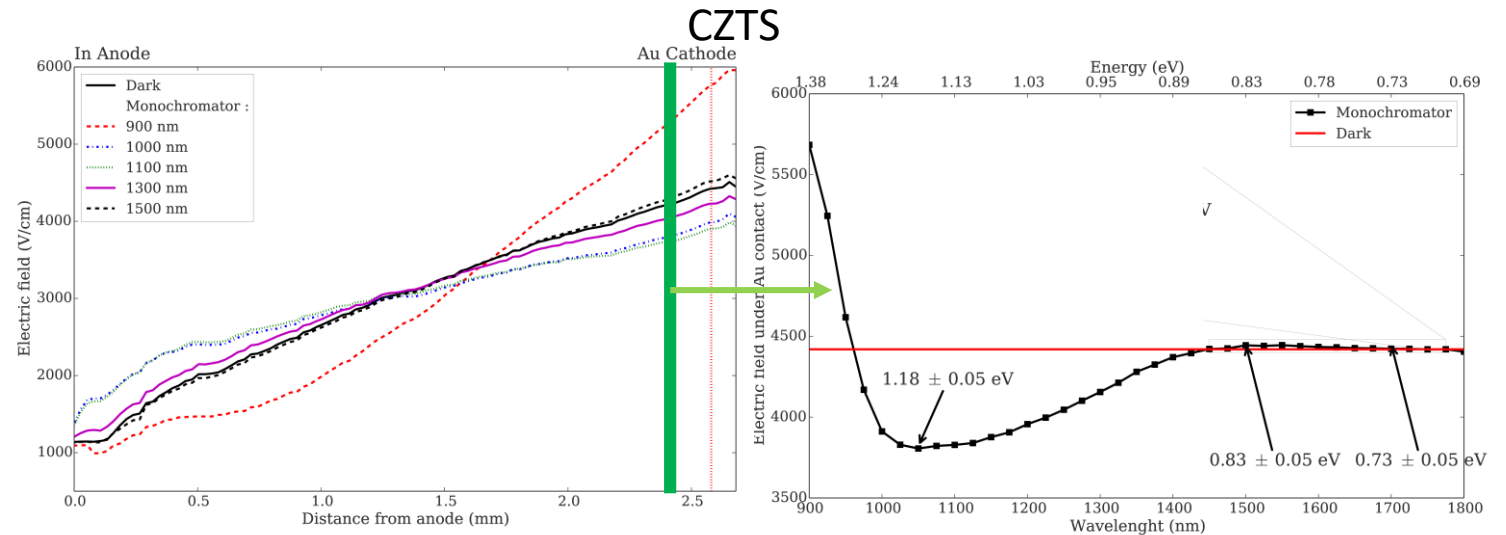
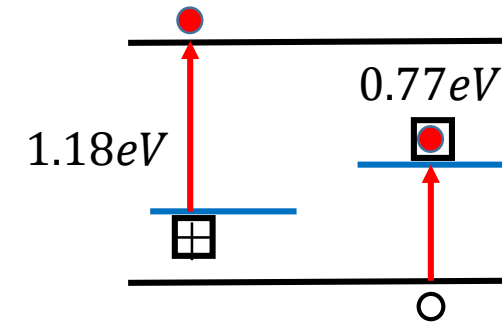
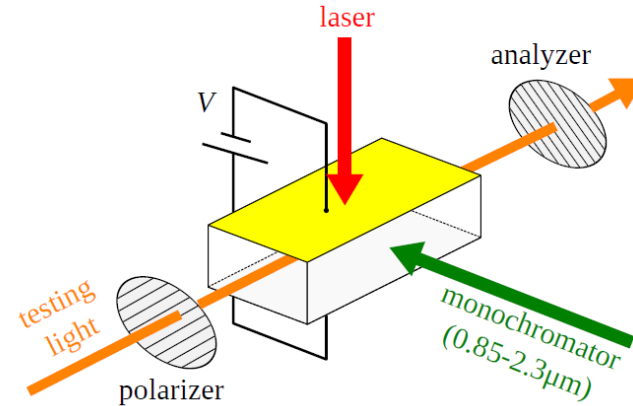


Experimental methods based on Pockels effect II

3-lights experiment

(infrared spectral scanning)

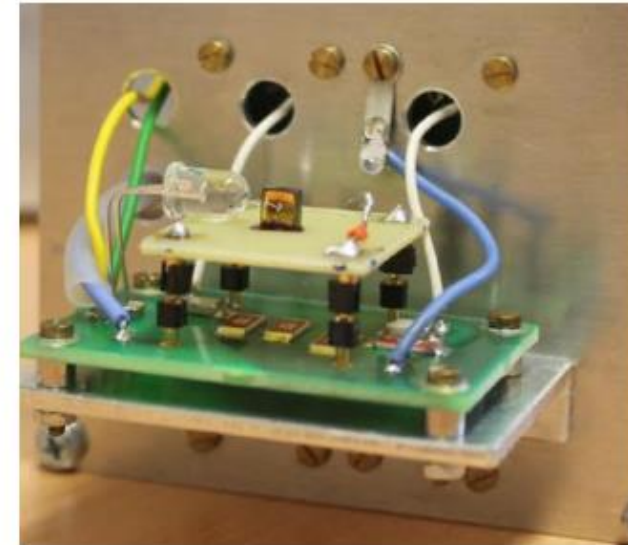
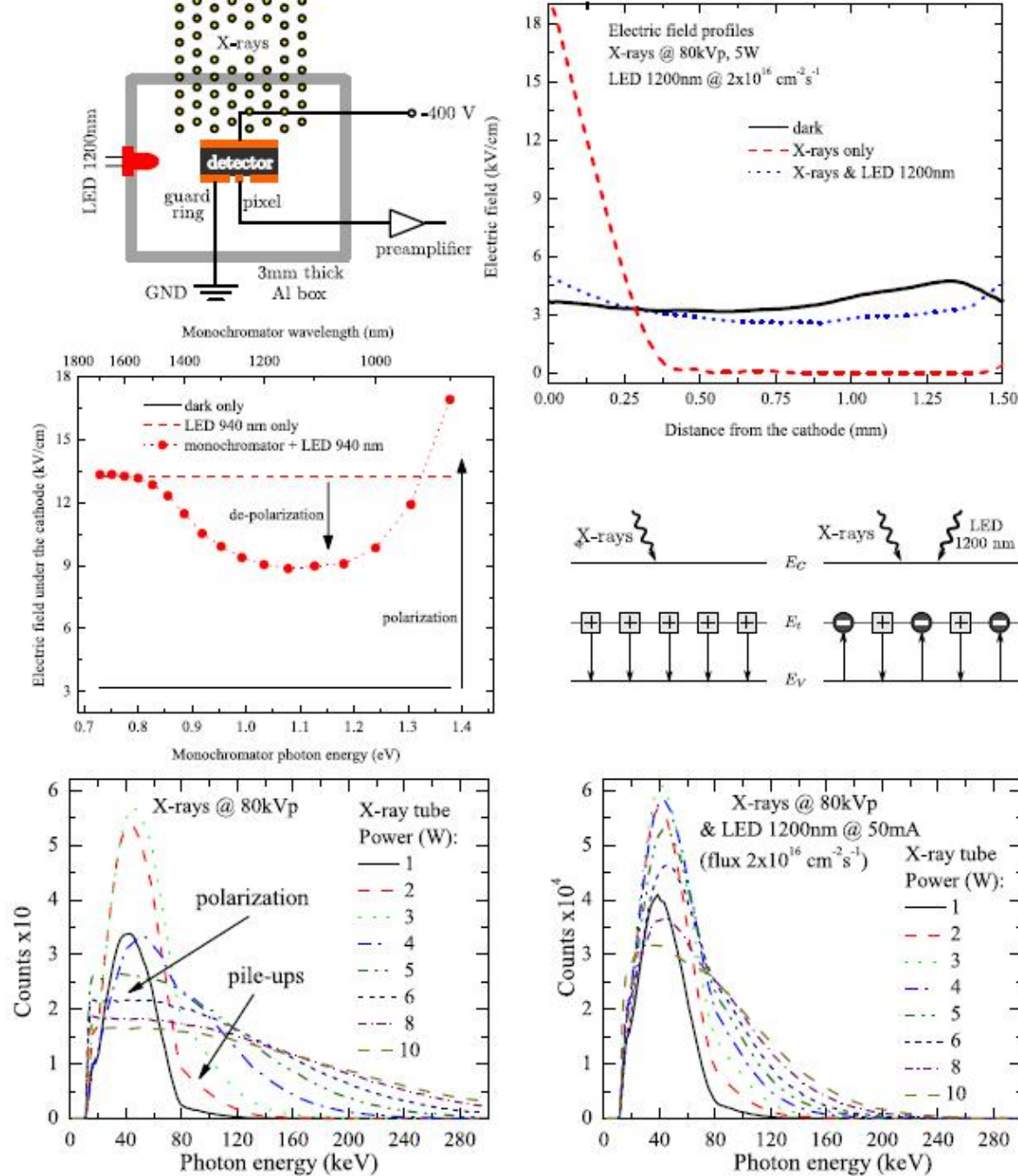
- Subject of study: optical transitions on deep levels
- Light sources:
 - Laser: band-to-band carrier generation (injection) \Rightarrow trap filling
 - Tunable monochromatic light: activation of optical transitions
 - Testing light: very low intensity, Pockels effect probe
- Output: E-field (charge) dependence on the photon energy reflecting the transitions enhanced by band-to-band generation (optical injection of carriers) \Rightarrow deep levels responsible for space charge accumulation
- Advantage: higher sensitivity than current techniques, direct space charge sign estimation



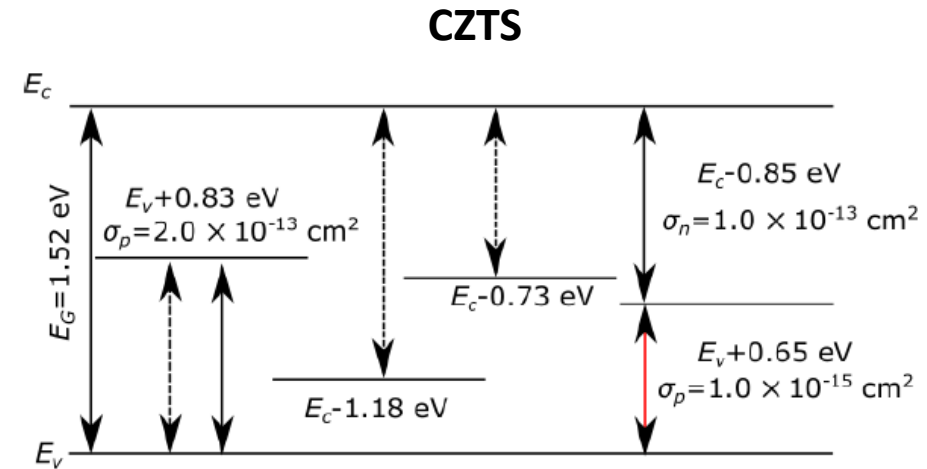
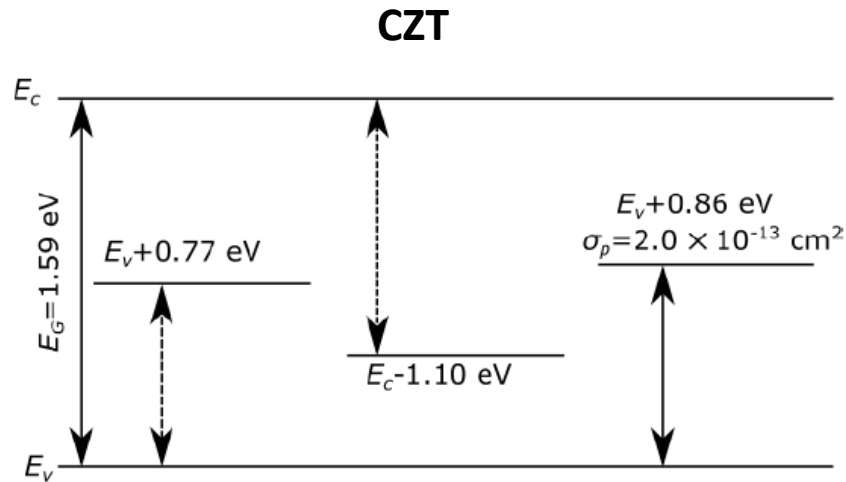
De-polarization at high fluxes

"De-polarization" of high-flux X-ray detector

- X-ray (tube at 80 kV) analogous e-h pair creation to band-to-band generation due to photoeffect
- significant positive space charge accumulation due to strong hole trapping \Rightarrow screening of the electric field (also "detector polarization") \Rightarrow reduction of CCE
- optical transition reducing space charge \Rightarrow detector recovery



Summary of deep levels

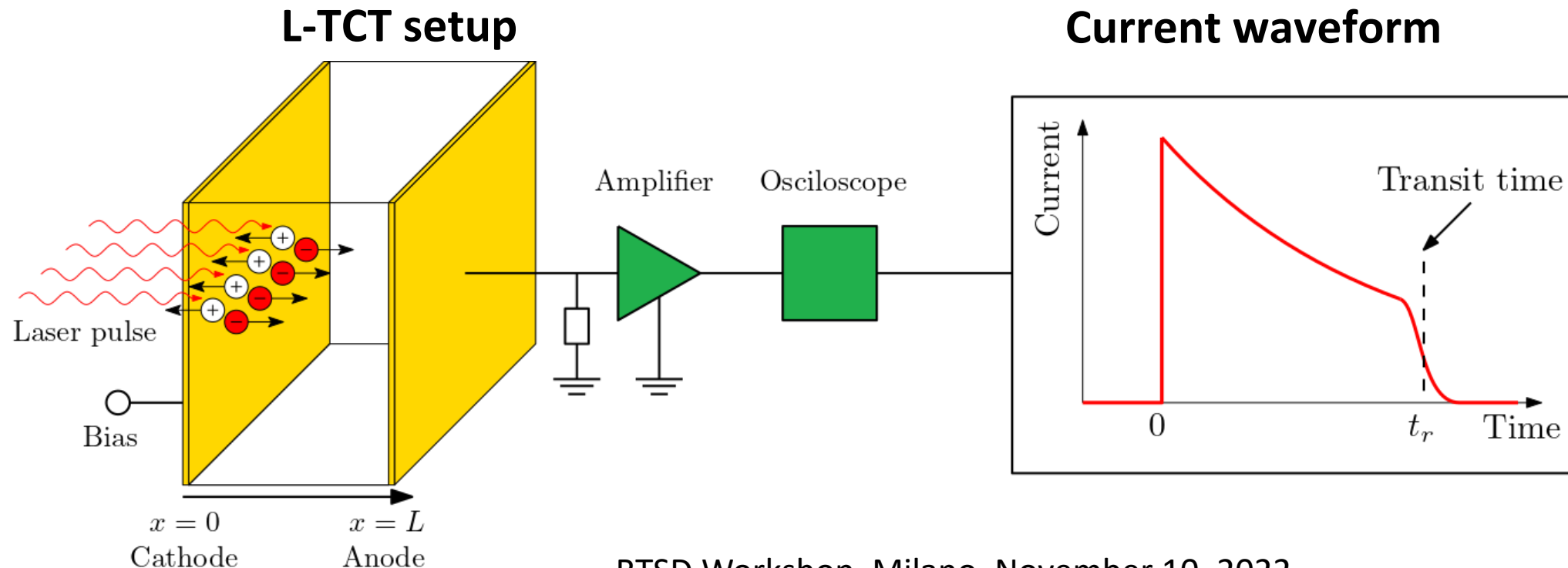


- ☐ Solid line – Time and temperature measurement
- ☐ Dashed line – Infrared spectral scanning
- ☐ Red line – Time and temperature current measurement

- ☐ $E_c - 1.10$ (1.18) eV - causes optically induced polarization (Te inclusions/precipitates or Te vacancy)
- ☐ $E_v + 0.83$ eV (CZTS) probably same origin as $E_v + 0.77$ eV (CZT) (Cd vacancy)
 - ☐ The energy shift was theoretically predicted by Varley [1]
- ☐ $E_c - 0.85$ eV (CZTS) – responsible for positive space charge
- ☐ $E_v + 0.86$ eV (CZT) - responsible for negative space charge

Laser Induced Current Technique (L-TCT)

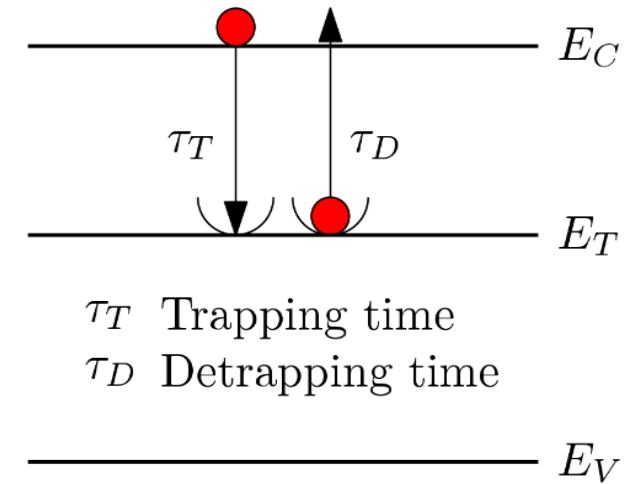
- Based on measuring the current response of the detector to a laser pulse
- Allows to characterize the charge transport (mobility, lifetime, electric field profile)
- Bias polarity selects which carrier type drift through detector



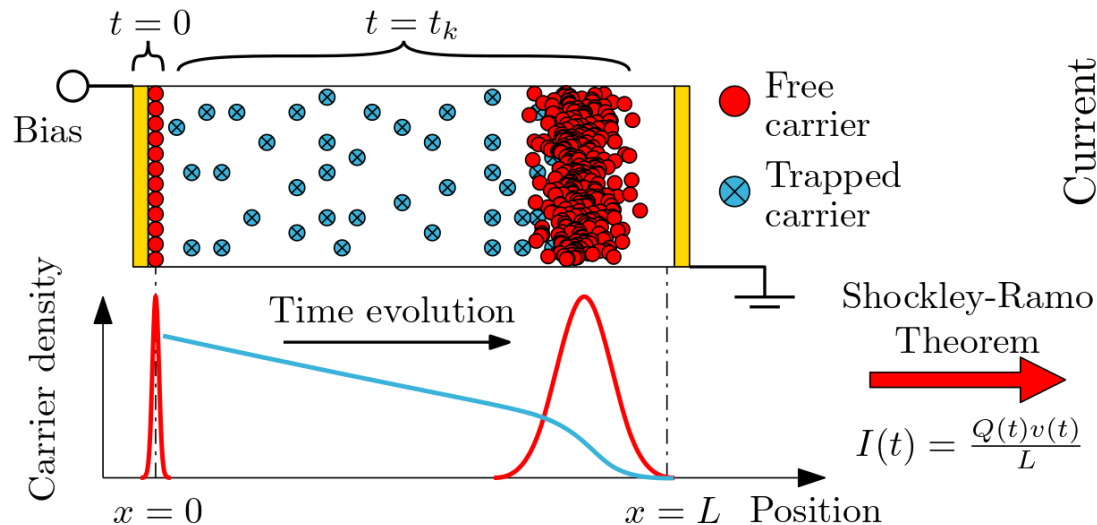
Monte Carlo Simulation

- 1D numerical simulation of charge transport in semiconductor detector
- Combined with numerical solution of drift-diffusion equation and Poisson's equation
- allows study of charge transport and space charge dynamics

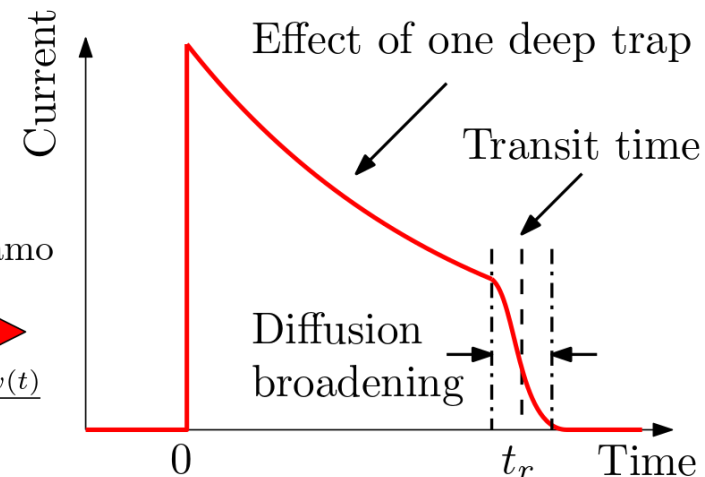
Band diagram



Detector

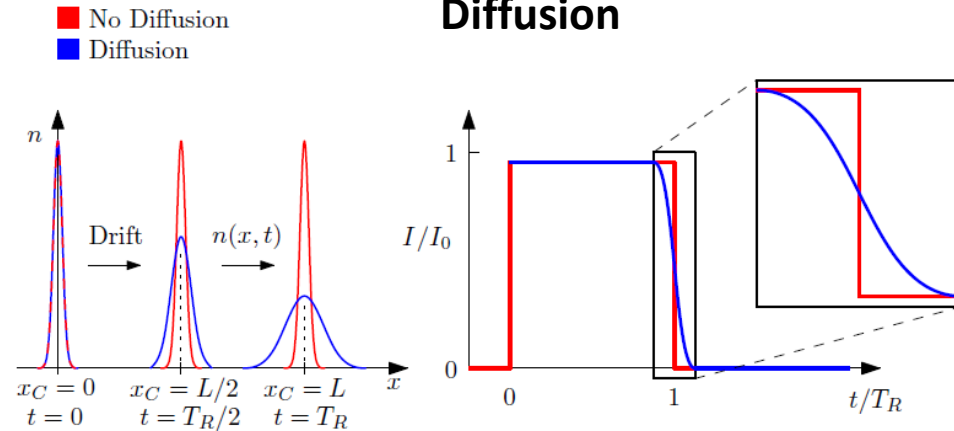


Current response

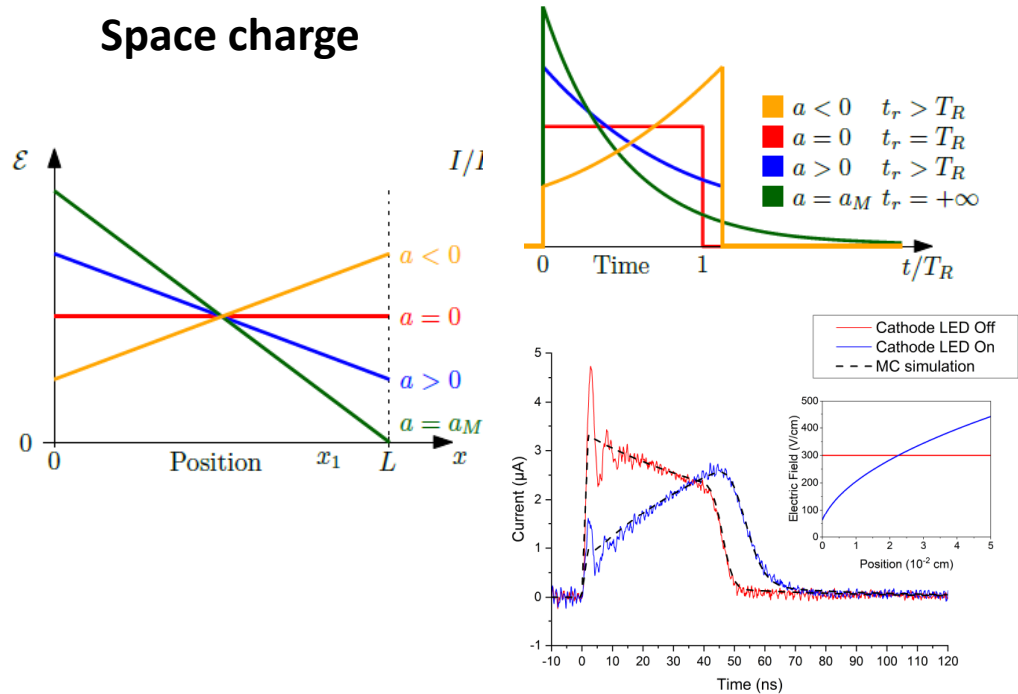


Effects influencing current waveform

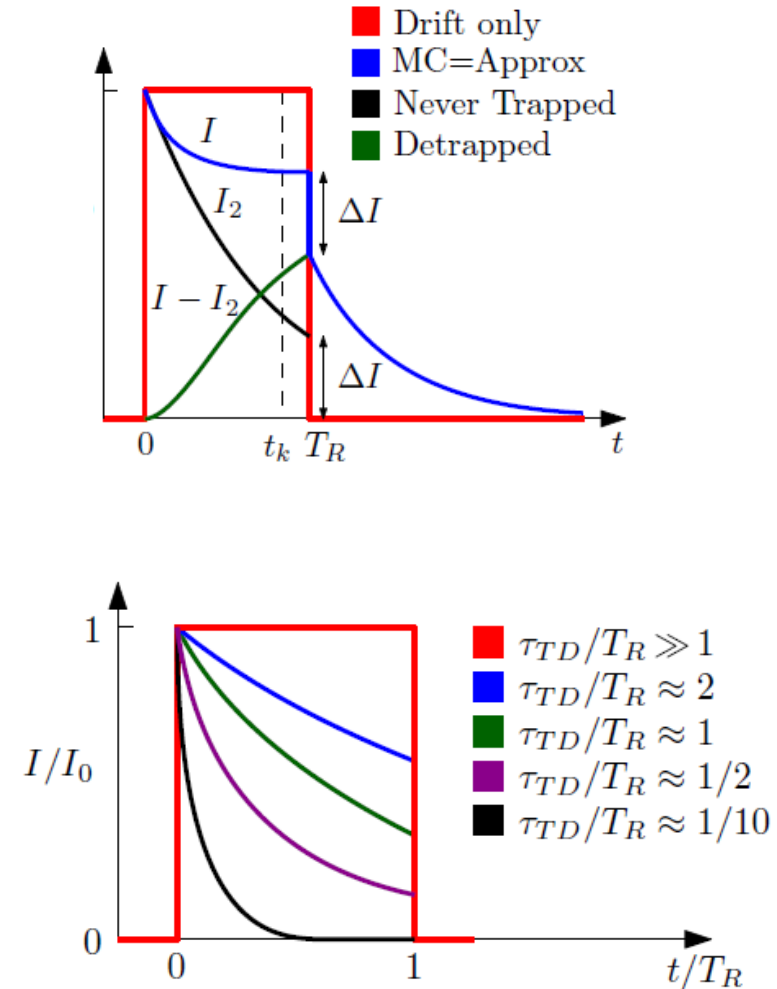
Diffusion



Space charge

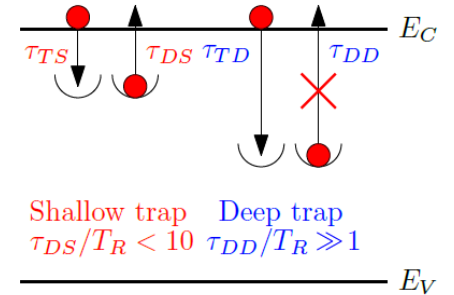


Trapping and de-trapping



$$\tau_T = \frac{1}{N_T \sigma_c v_{th}}$$

$$\tau_D = \frac{1}{N_C \sigma_c v_{th}} \exp\left(\frac{E_T}{k_B T}\right)$$

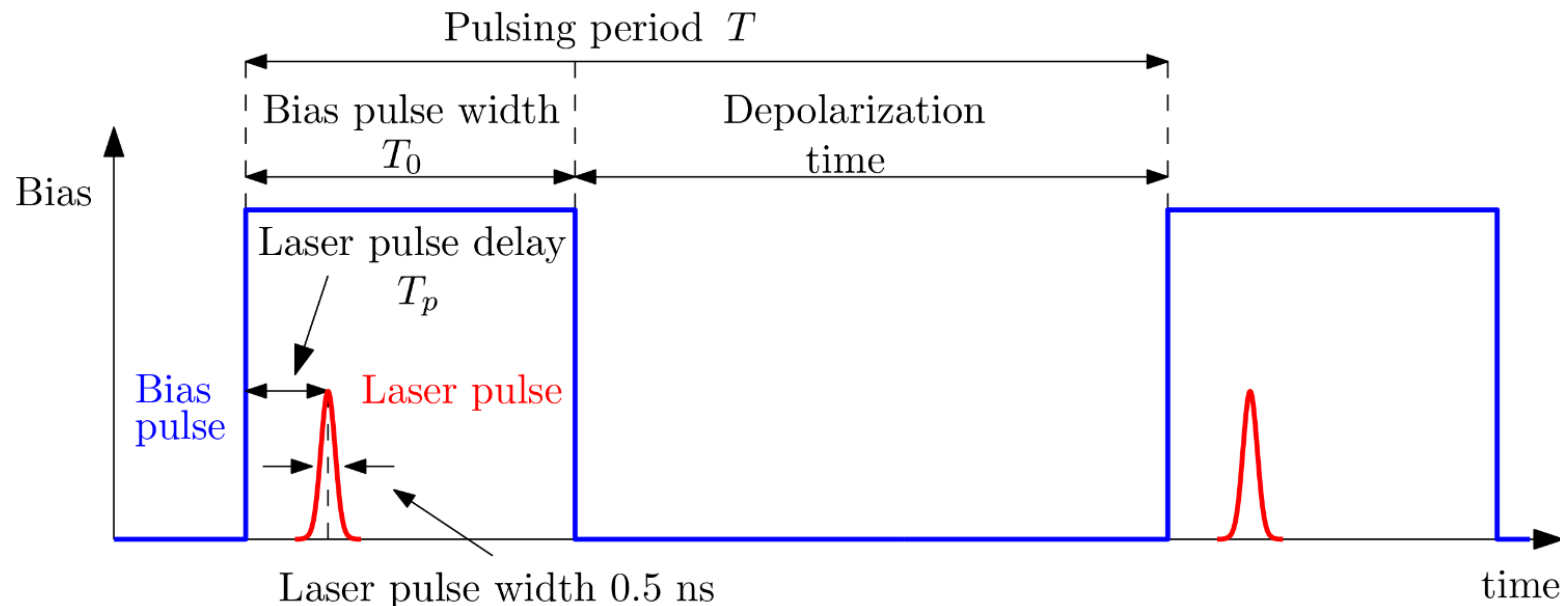


Shallow trap $\tau_{DS}/T_R < 10$ Deep trap $\tau_{DD}/T_R \gg 1$

Space charge elimination

- Space charge deteriorates detector performance
- Without bias the detector is neutral
- Space charge formation starts after bias application
- Space charge can be eliminated using **pulsed bias** and effects of space charge can be distinguished from effects of traps
- Changing the laser pulse delay allows study of space charge evolution

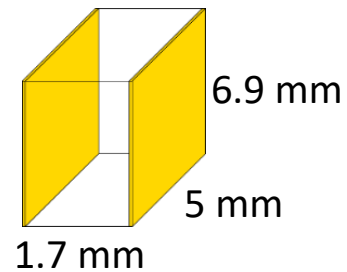
Synchronization of laser pulse and bias pulse



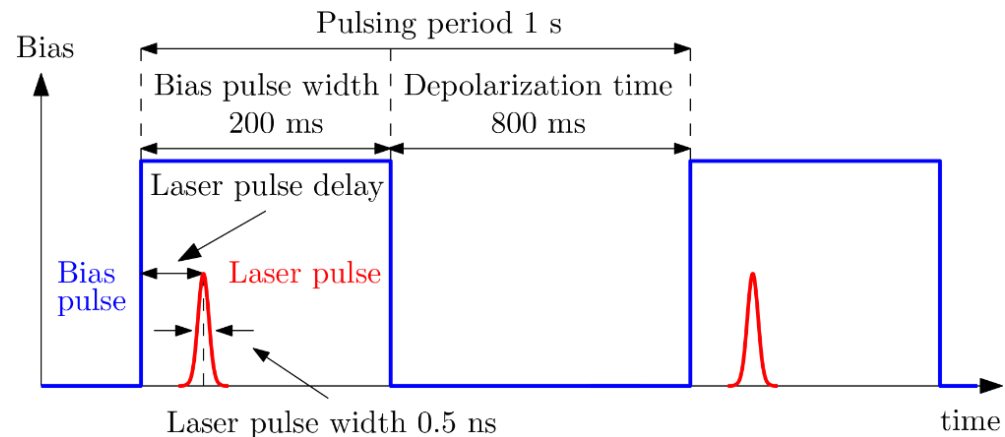
CdZnTeSe - L-TCT measurement results

- Semi-insulating p-type $\text{Cd}_{0.9}\text{Zn}_{0.1}\text{Te}_{0.96}\text{Se}_{0.04}$ sample is used
- L-TCT is combined with pulsed bias to study space charge dynamics

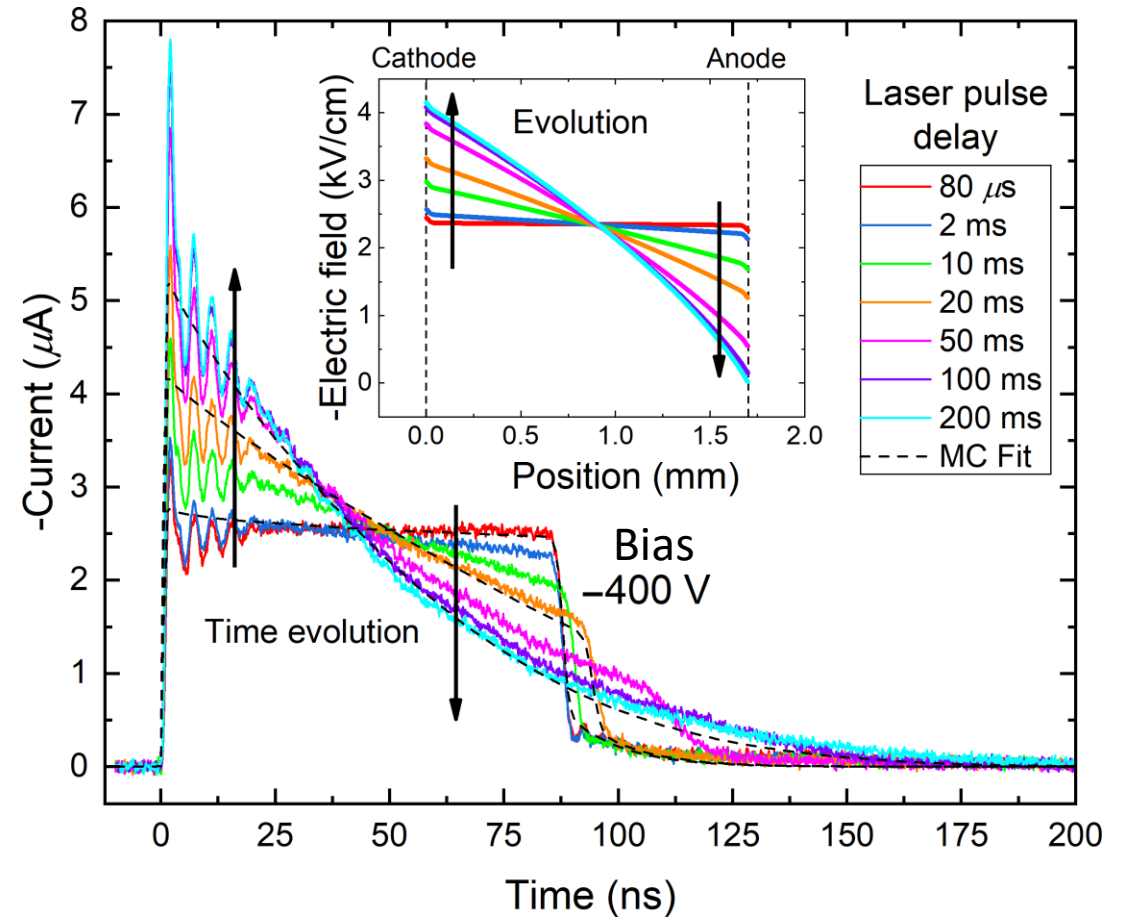
Sample geometry



Synchronization of laser pulse and bias pulse



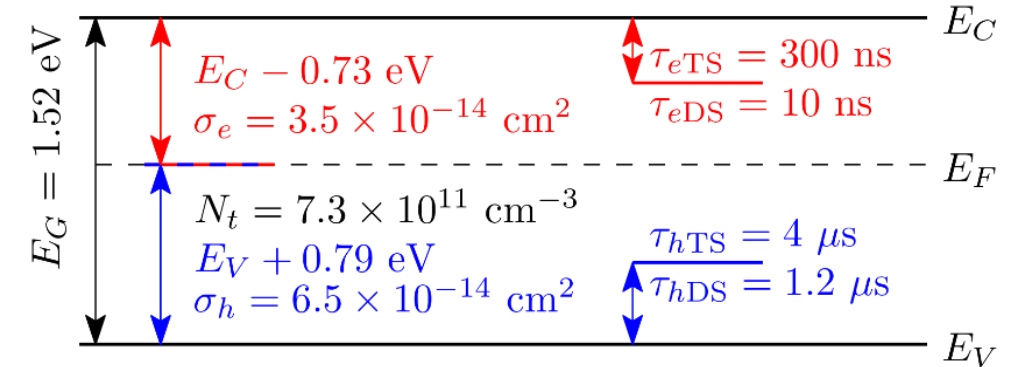
Electron-current waveforms



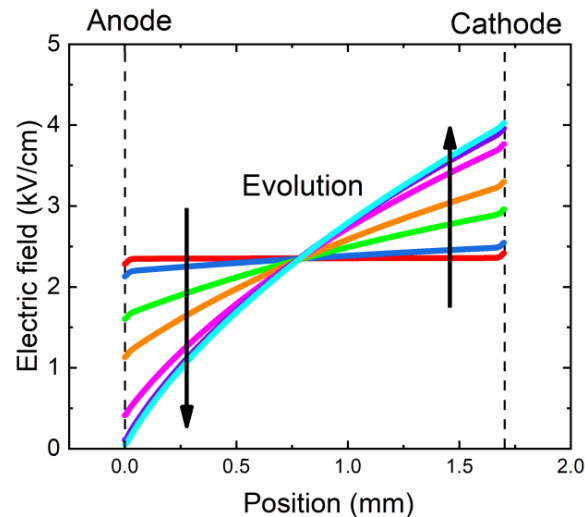
Space charge dynamics

- Three defect levels are sufficient to describe all observed effects
- Positive space charge forms due to hole injection from anode combined with **recombination level** near Fermi level
- Shallow levels do not contribute to space charge

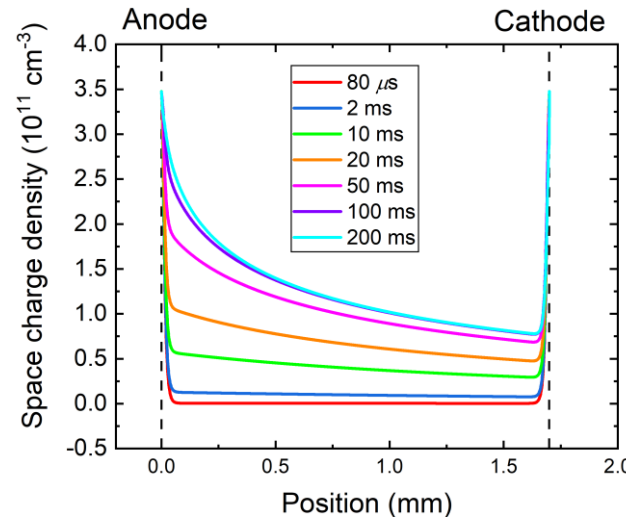
Band diagram



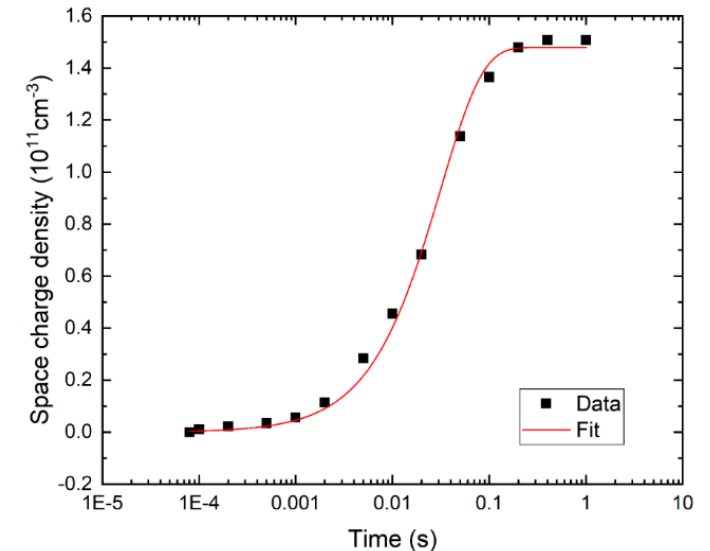
Electric field profile



Space charge profile



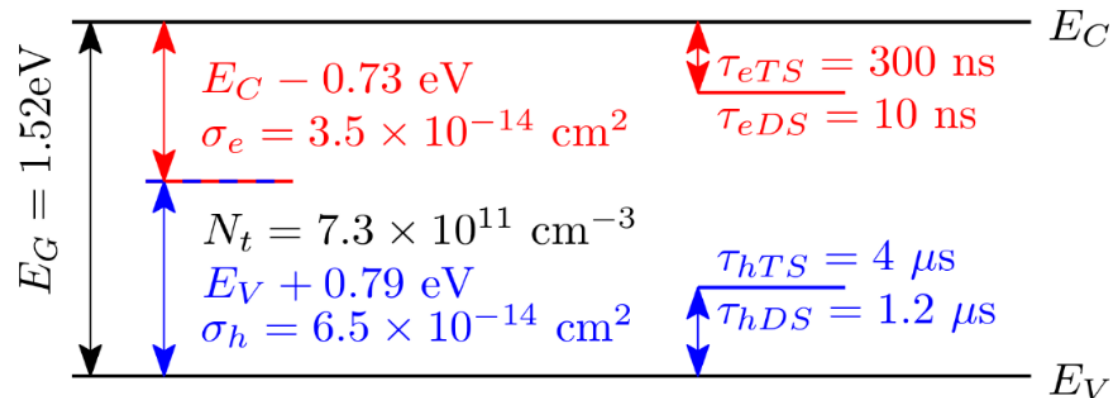
Mean space charge evolution



Evaluated parameters

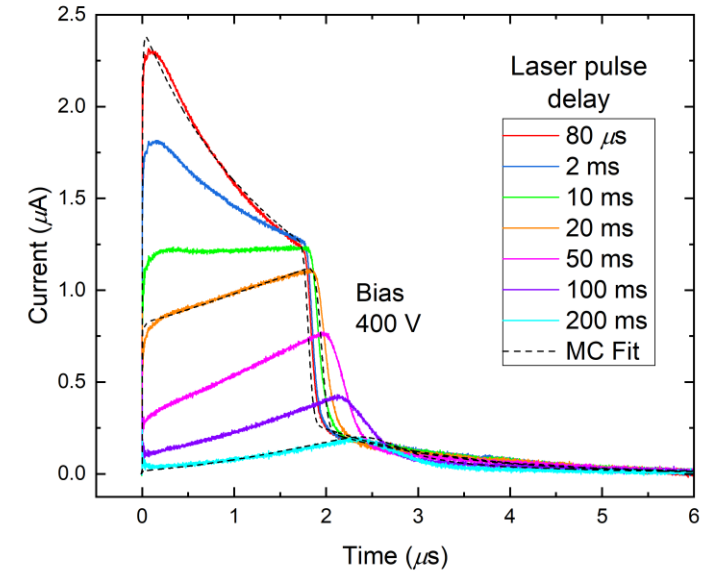
- Same experiment was measured with positive bias for holes
- Identical electric field profile is obtained
- **Evaluated parameters are:**
 - Electron mobility $\mu_e = 830 \text{ cm}^2/\text{Vs}$
 - Hole mobility $\mu_h = 40 \text{ cm}^2/\text{Vs}$
 - Electron lifetime $\tau_e = 2.3 \text{ }\mu\text{s}$
 - Hole lifetime $\tau_h = 3.6 \text{ }\mu\text{s}$
 - Three defect levels:

Band diagram

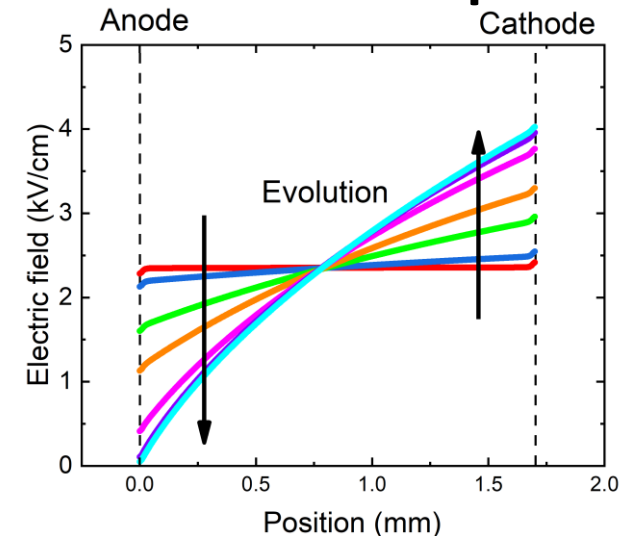


RTSD Workshop, Milano, November 10, 2022

Hole-current waveforms



Electric field profile



Origin of deep levels

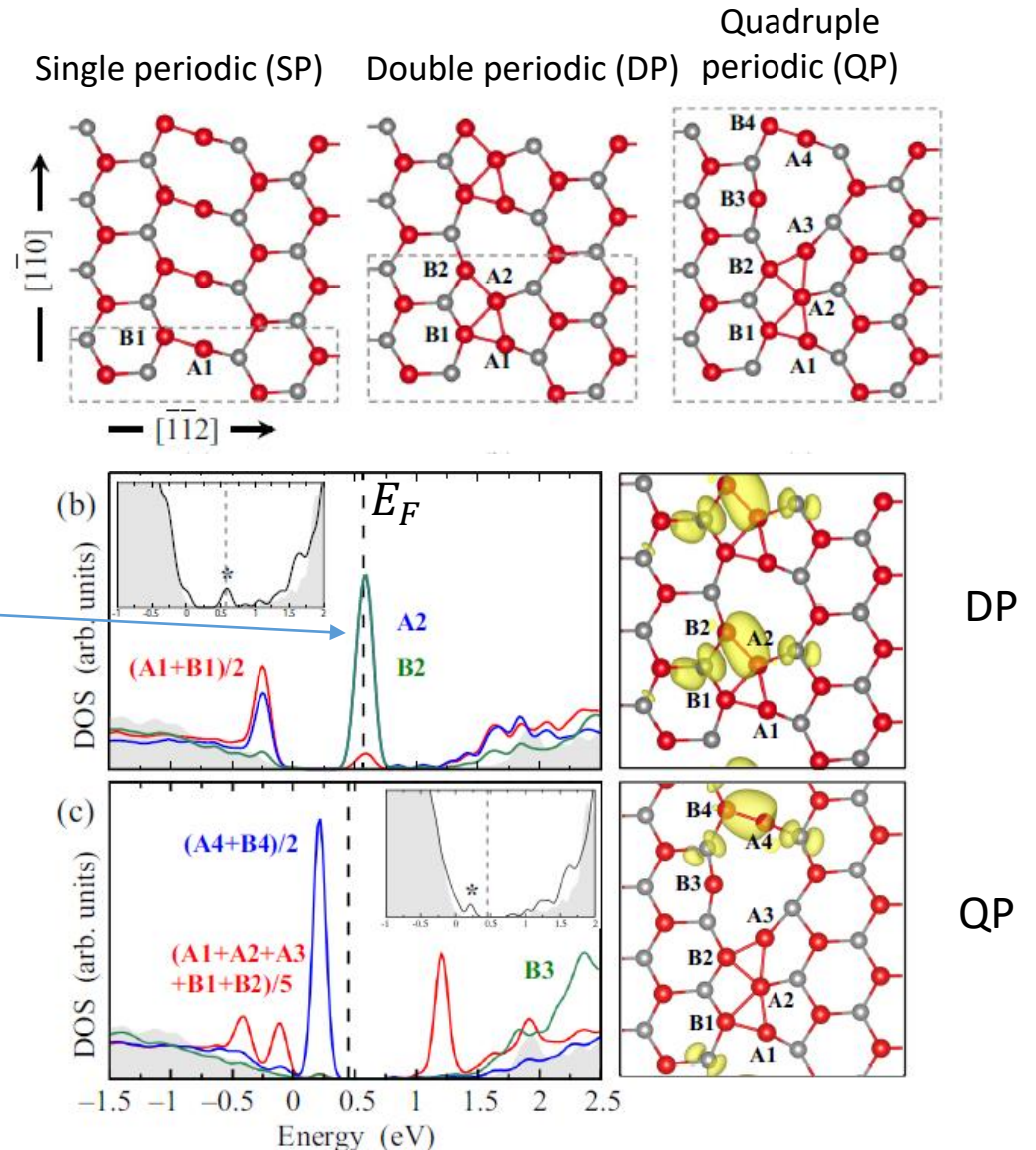
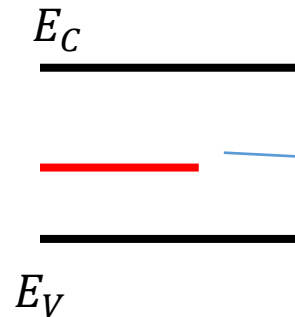
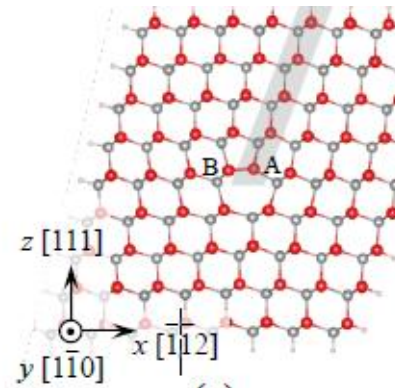
60° Cd core glide dislocation in the (111) plane – first principles calculations

Due to a small concentration of deep levels is an experimental investigation of their origin difficult

Possible sources:

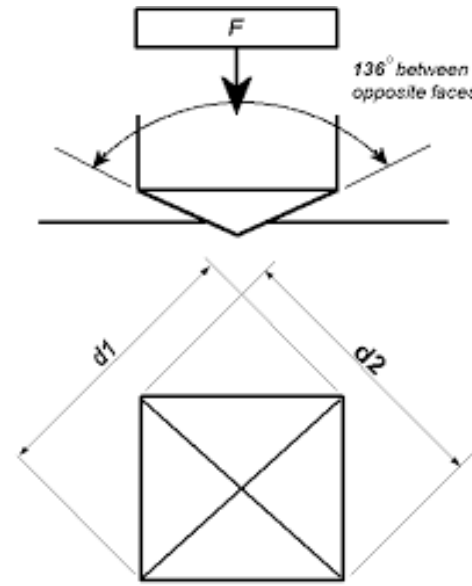
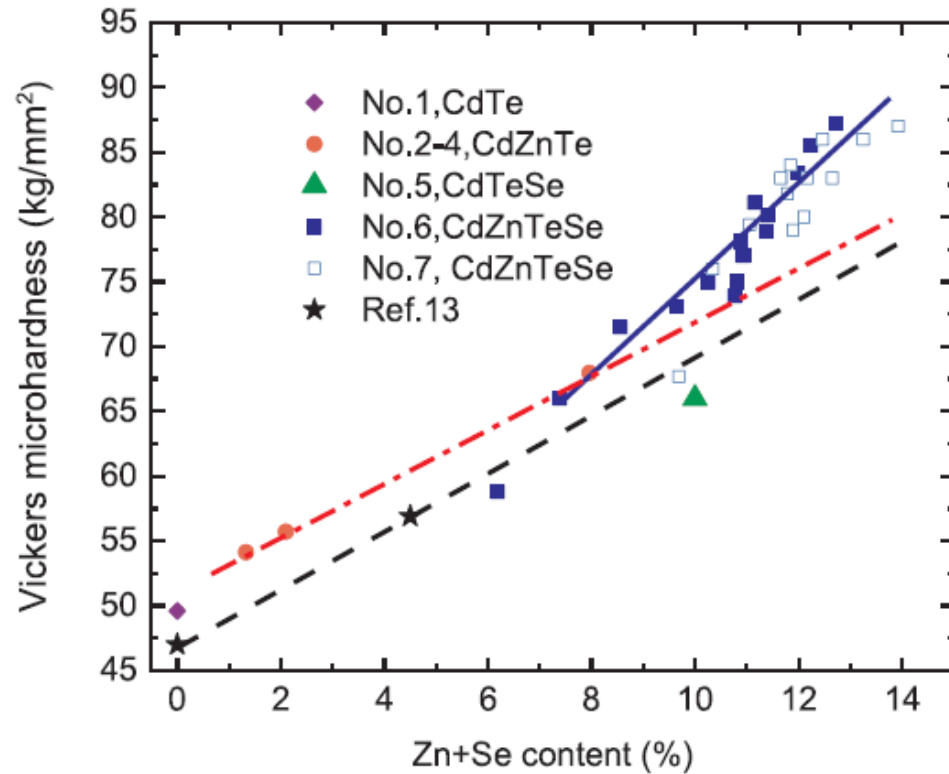
- Native defects and their complexes (V_{Cd}, Te_{Cd}, \dots)
- Impurities
- dislocations

Theoretical calculations of DOS show that dislocation-related deep levels can act as recombination and trapping centers and their position in the gap agree with experiment.

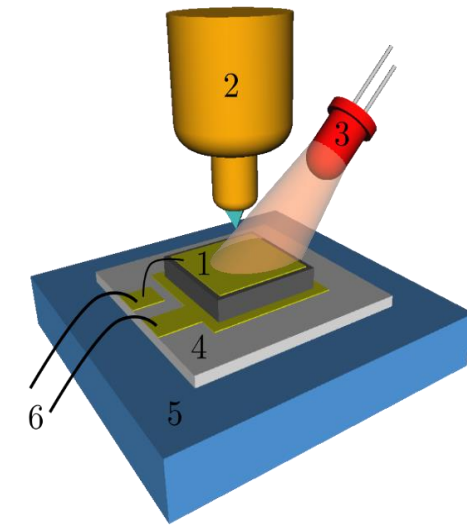


Kweon K.A, Aberg A., Lordi V., Phys. Rev. B 93 (2016) 174109,
<https://doi.org/10.1103/PhysRevB.93.174109>

Vickers microhardness



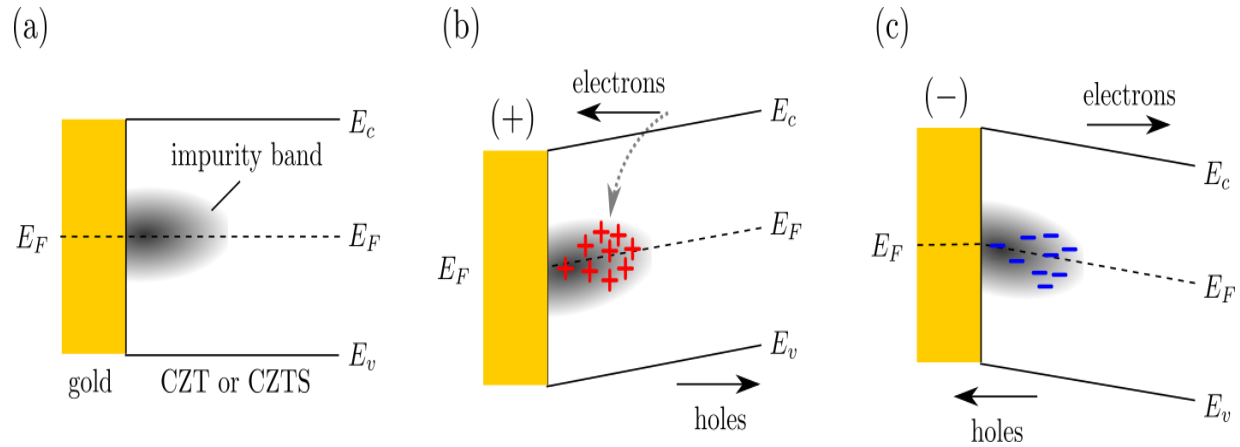
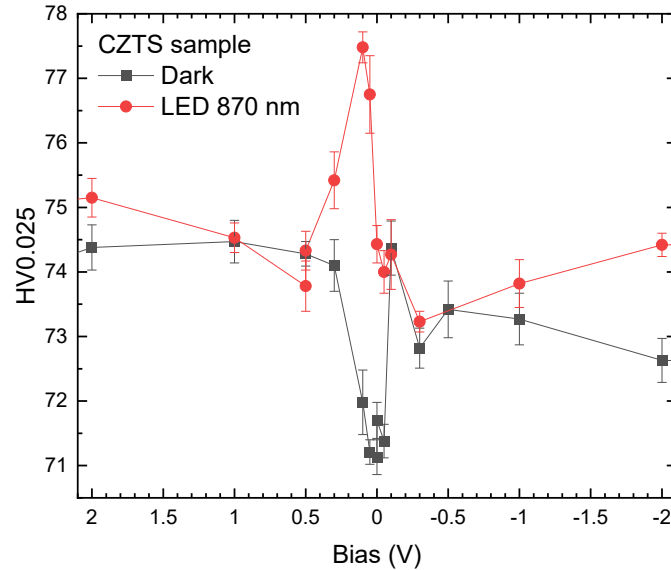
LED or white laser
with bandpass filter



This result shows that Se plays a major role in an effective solution hardening of the CZTS matrix and indicates a possible additional strengthening of the effect when Zn and Se are mixed in the CdTe lattice.

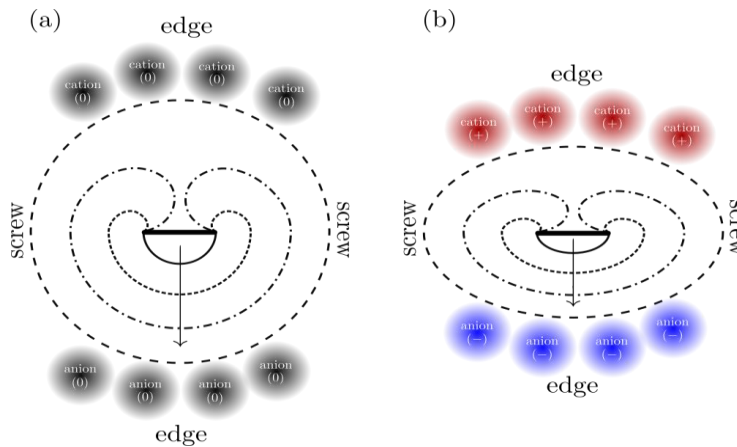
Modified setup – measurement of microhardness with illumination and/or applied bias

Bias dependence of photo plasticity



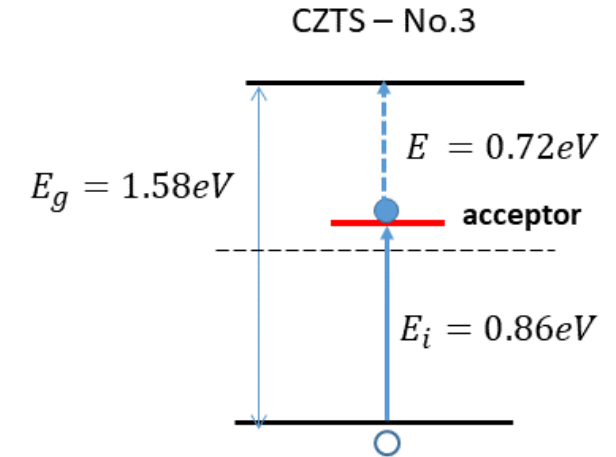
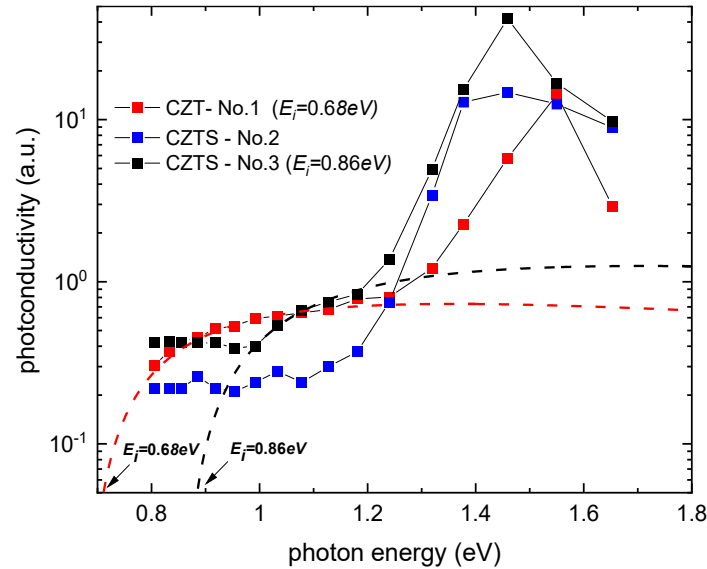
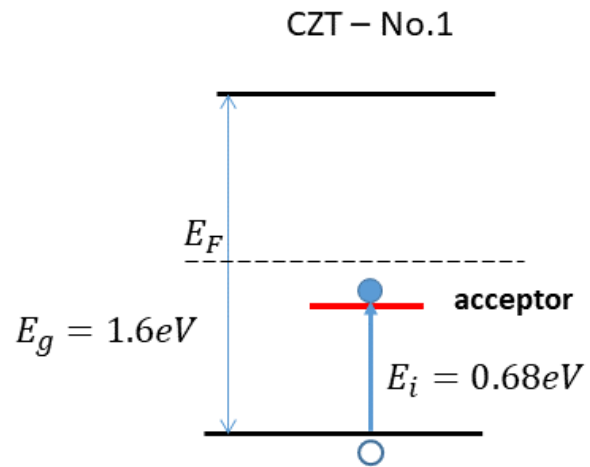
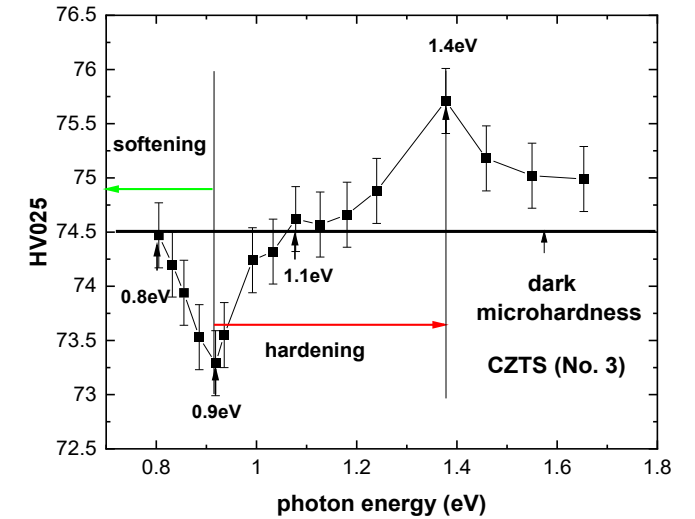
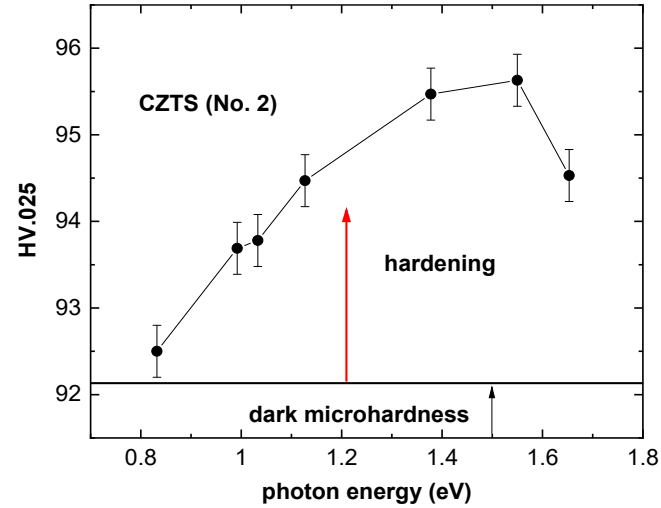
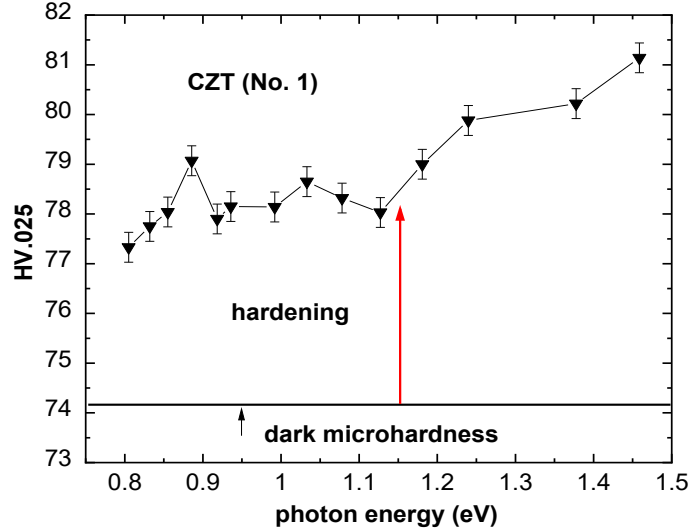
Illuminating the sample leads to the generation of an excessive amount of free carriers that can be captured by dislocation segments according to their electrical character, resulting in dislocation reconstruction and ensuing hardening of the material

In the case of an applied bias, the deformation-induced defect states are filled by the charges from the adjacent contact, while the opposite charge is not supplied by the bulk. One of the charge types (positive/negative) starts to dominate the other one. Subsequently, only appropriate dislocation segments may pass the reconstruction. Due to this reason, the hardness stabilizes near the middle of the hardness at 0 V in the dark and for the illumination



The cation-rich and anion-rich regions accumulate at the opposite sides of the dislocation source. Uncharged dislocations outlined in the left panel (a) glide more easily than charged dislocations shown in the right panel

Spectral dependence of photo plasticity



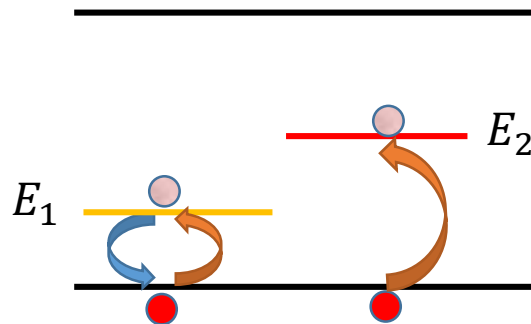
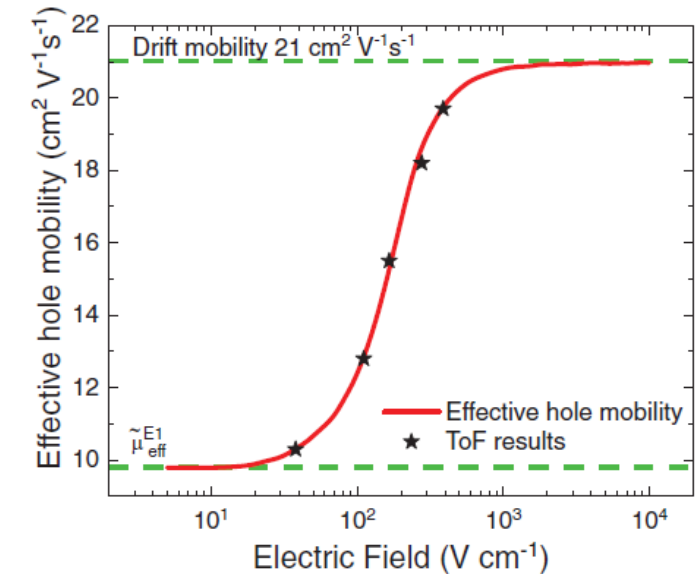
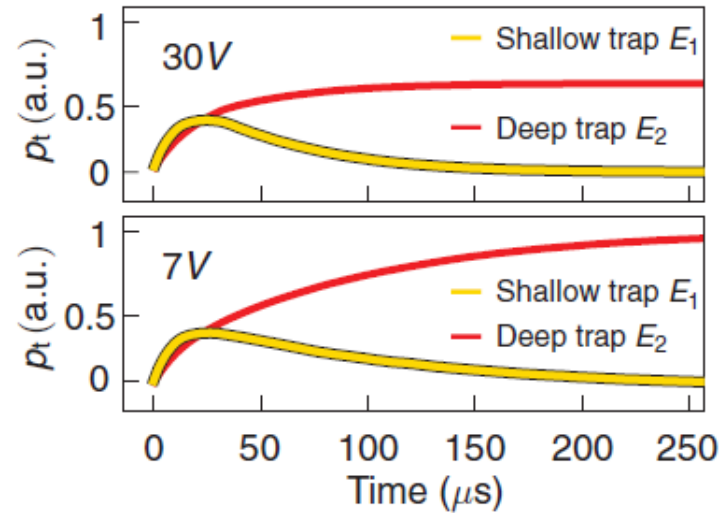
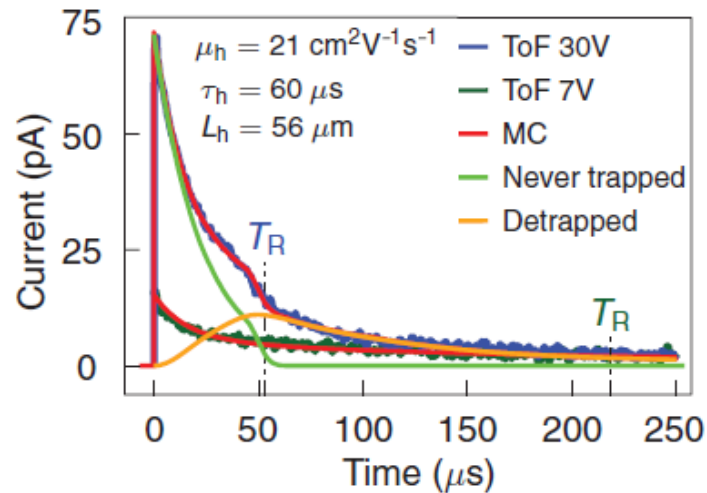
Defects in hybrid perovskites

Methylammonium halide perovskites, MAPbI₃, MABrI₃

Materials with large application potential – photovoltaics, LED, FET, X-ray and gamma-ray detection

Issues to be solved - stability and defect control

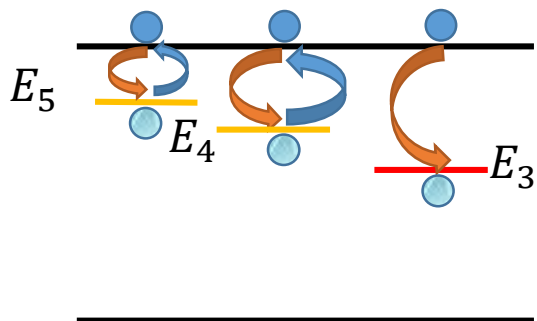
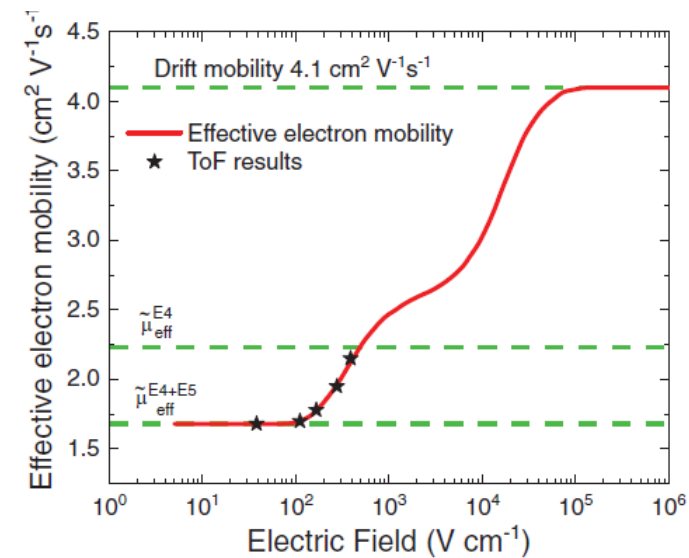
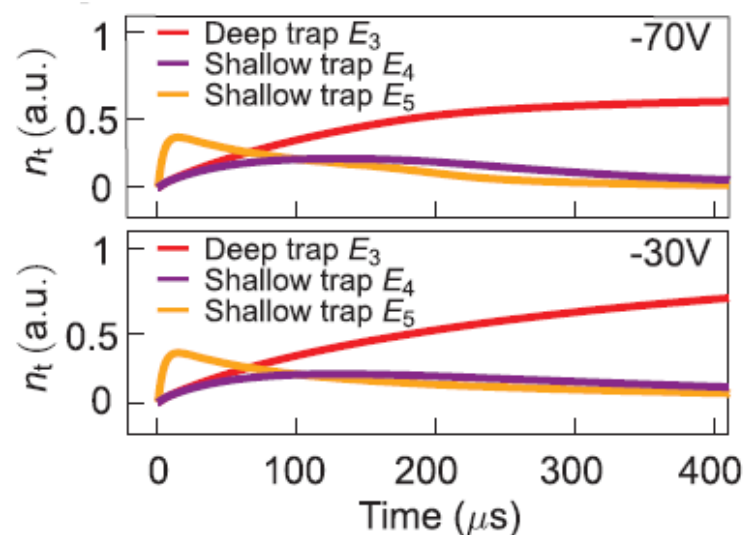
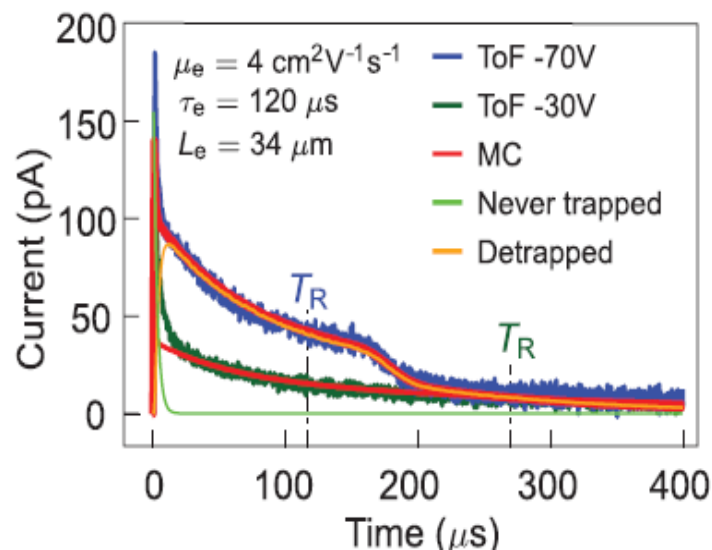
Hole transport MAPbI₃ – TCT method



E_1 is responsible for fast trapping ($\tau_t = 3.5\mu\text{s}$) and de-trapping ($\tau_t = 4\mu\text{s}$) resulting in reduction of effective hole mobility $\mu_{eff} = \frac{\mu_e}{1 + \frac{\tau_D}{\tau_t}}$

E_2 permanently traps free holes ($\tau_t = 60\mu\text{s}$, $\tau_D \gg 20\text{ms}$) resulting in reduction of effective hole mobility

Electron transport MAPbI₃ – TCT method

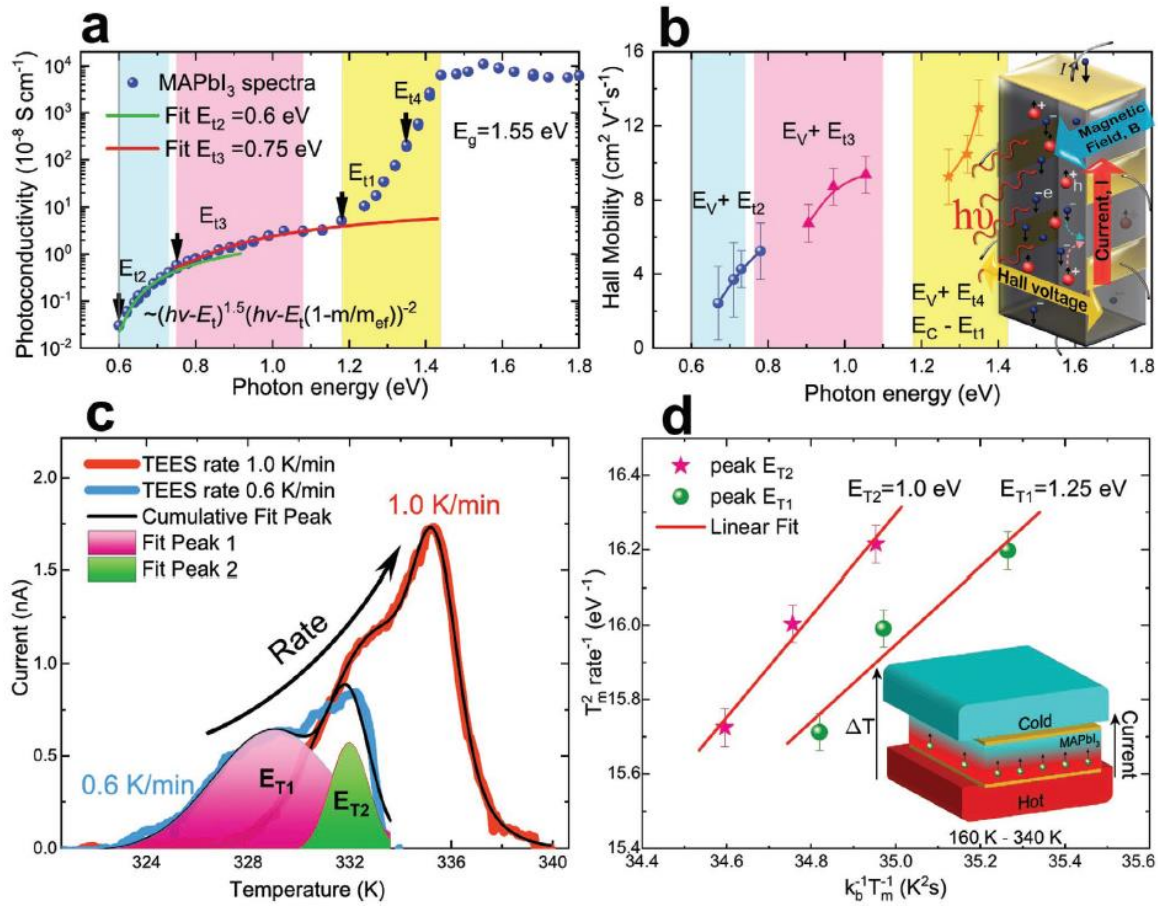


E_4 and E_5 are responsible for fast trapping

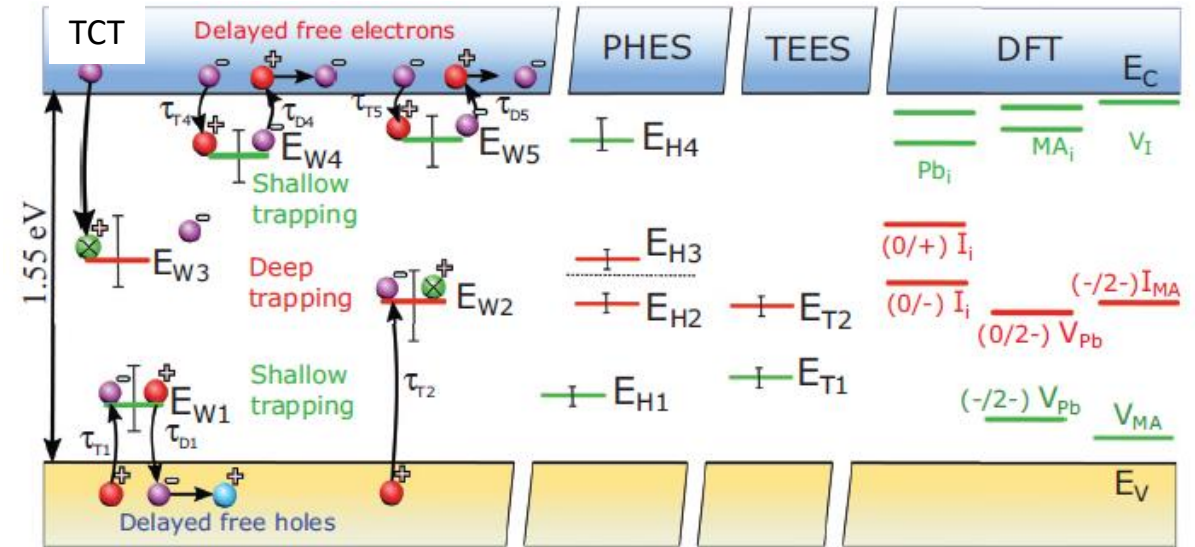
$$\mu_{eff} = \frac{\mu_e}{1 + \frac{\tau_{D4} + \tau_{D5}}{\tau_{t4} + \tau_{t5}}}$$

E_3 permanently traps free electrons ($\tau_t = 120 \mu\text{s}$, $\tau_D \gg 20 \text{ ms}$) resulting in reduction of effective hole mobility

Deep levels in MAPbI₃ – summary



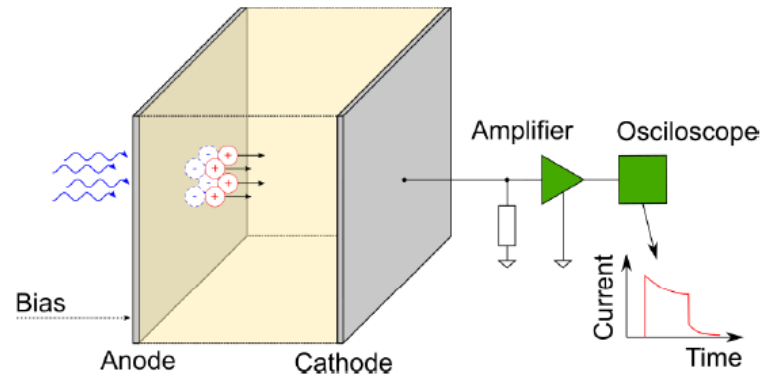
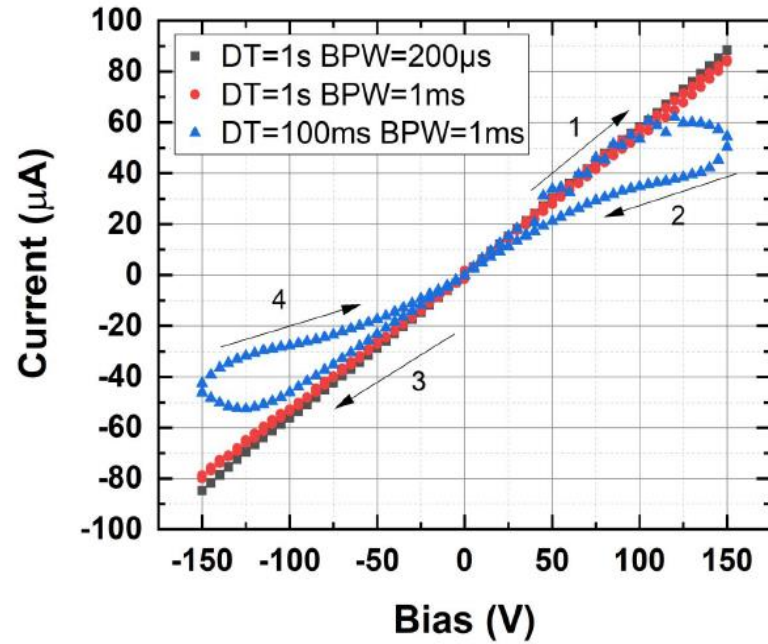
TCT - transient current technique
 PHES - photo Hall effect spectroscopy
 TEES – thermoelectric effect spectroscopy
 DFT – density functional theory



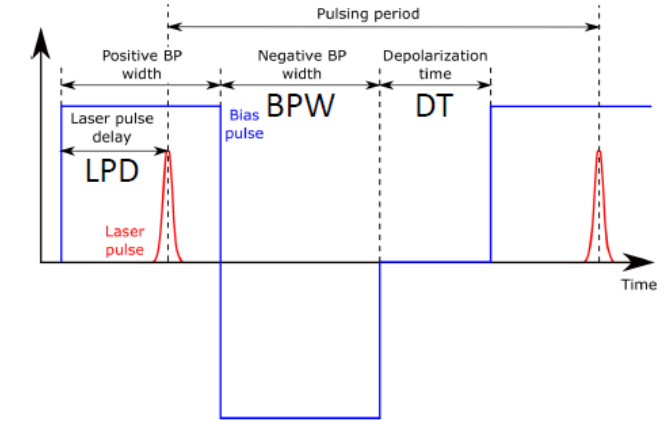
A. Musiienko, D.Cerrati, J. Pipek et al, Adv. Func. Mat. 2021, 31, 2104467

RTSD Workshop, Milano, November 10, 2022

Space charge formation and relaxation in MAPbBr₃



Scheme of our L-TCT setup

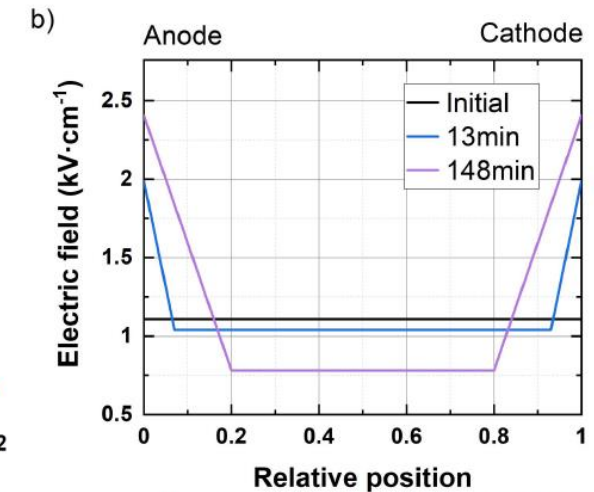
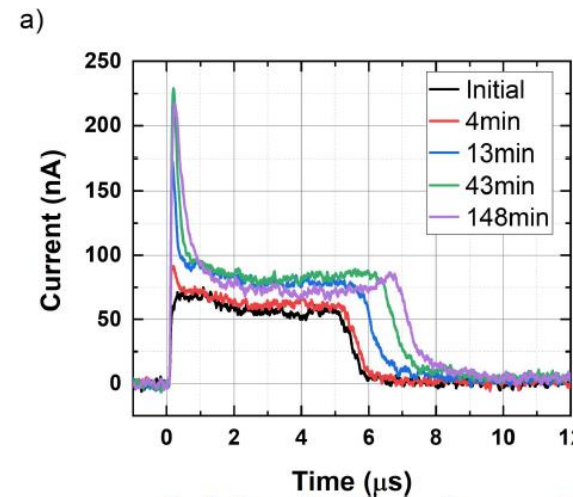


Laser and bias pulse synchronization

Polarization effects observed

Two models to explain:

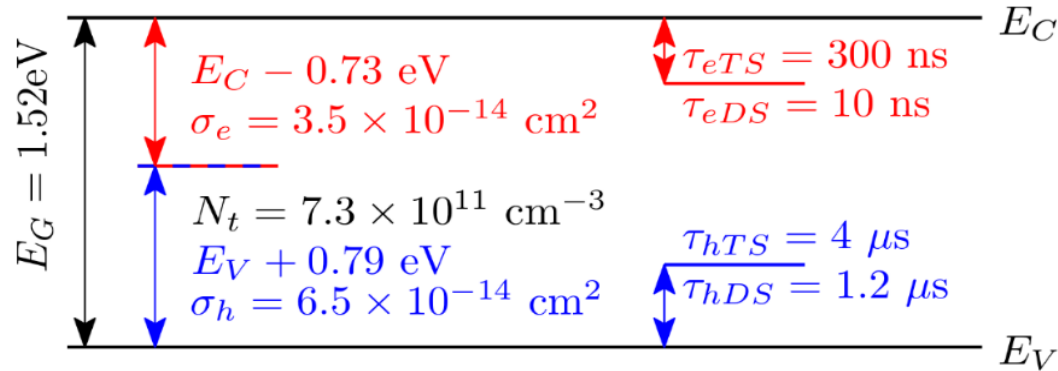
1. Ion migration
2. Trapping of carriers at deep levels



Evolution of hole waveforms and b) corresponding electric field for 100V, DT=100ms, BPW=1ms and LPD=100 μs .

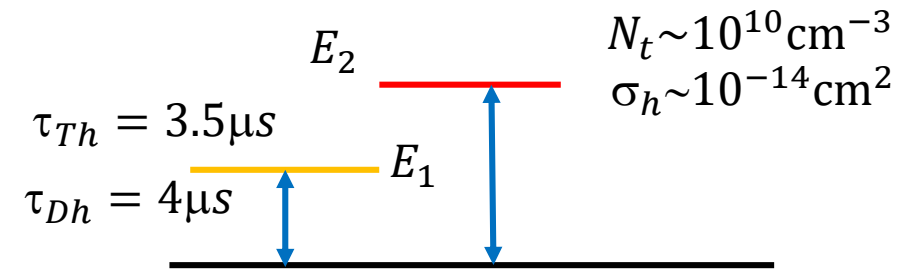
Level comparison

CdZnTeSe group



$$\mu_{eff,e} = \frac{\mu_e}{1 + \frac{\tau_D}{\tau_t}} = \frac{\mu_e}{1 + \frac{10}{300}} = 0.967 \mu_e$$

MAPbI₃



$$\mu_{eff,h} = \frac{\mu_e}{1 + \frac{\tau_D}{\tau_t}} = \frac{\mu_e}{1 + \frac{4}{3.5}} = 0.467 \mu_e$$

Midgap level - similar concentration, trapping activity potentially leading to polarization

Shallow traps – in both cases the effective mobility is decreased by trapping at de-trapping at deep levels. The effect is stronger in measured perovskites samples

Future work

Development of L-TCT setup (temperature dependence measurements) and its applications to perovskites, CdTe group compounds, and other materials

Development of Pockels effect method - measurements of graphene/SiC structures, perovskites etc.

Continue to study mechanical properties – Vickers indentation, AFM - CdTe group, perovskites

Thank you very much for your attention